remote sensing

MDPI

Article

Exploring Trends and Variability of Water Quality over Lake Titicaca Using Global Remote Sensing Products

Vann Harvey Maligaya [1,*], Analy Baltodano [1], Afnan Agramont [1,2] and Ann van Griensven [1,3]

[1] Water and Climate Department, Vrije Universiteit Brussel, 1050 Brussels, Belgium; baltodano.martinez.analy@vub.be (A.B.); afnan.agramont.akiyama@vub.be (A.A.); ann.van.griensven@vub.be (A.v.G.)
[2] Centro de Investigación en Agua Energía y Sostenibilidad, Universidad Católica Boliviana San Pablo, La Paz 4805, Bolivia
[3] Core of Hydrology and Water Resources, UNESCO-IHE Institute for Water Education, 2611 AX Delft, The Netherlands
* Correspondence: vannharveymaligaya@gmail.com

Abstract: Understanding the current water quality dynamics is necessary to ensure that ecological and sociocultural services are provided to the population and the natural environment. Water quality monitoring of lakes is usually performed with in situ measurements; however, these are costly, time consuming, laborious, and can have limited spatial coverage. Nowadays, remote sensing offers an alternative source of data to be used in water quality monitoring; by applying appropriate algorithms to satellite imagery, it is possible to retrieve water quality parameters. The use of global remote sensing water quality products increased in the last decade, and there are a multitude of products available from various databases. However, in Latin America, studies on the inter-comparison of the applicability of these products for water quality monitoring is rather scarce. Therefore, in this study, global remote sensing products estimating various water quality parameters were explored on Lake Titicaca and compared with each other and sources of data. Two products, the Copernicus Global Land Service (CGLS) and the European Space Agency Lakes Climate Change Initiative (ESA-CCI), were evaluated through a comparison with in situ measurements and with each other for analysis of the spatiotemporal variability of lake surface water temperature (LSWT), turbidity, and chlorophyll-a. The results of this study showed that the two products had limited accuracy when compared to in situ data; however, remarkable performance was observed in terms of exhibiting spatiotemporal variability of the WQ parameters. The ESA-CCI LSWT product performed better than the CGLS product in estimating LSWT, while the two products were on par with each other in terms of demonstrating the spatiotemporal patterns of the WQ parameters. Overall, these two global remote sensing water quality products can be used to monitor Lake Titicaca, currently with limited accuracy, but they can be improved with precise pixel identification, accurate optical water type definition, and better algorithms for atmospheric correction and retrieval. This highlights the need for the improvement of global WQ products to fit local conditions and make the products more useful for decision-making at the appropriate scale.

Keywords: Lake Titicaca; water quality; remote sensing products; validation; spatiotemporal variability

Citation: Maligaya, V.H.; Baltodano, A.; Agramont, A.; van Griensven, A. Exploring Trends and Variability of Water Quality over Lake Titicaca Using Global Remote Sensing Products. *Remote Sens.* **2024**, *16*, 4785. https://doi.org/10.3390/rs16244785

Academic Editors: Emanuele Mandanici and Sara Kasmaeeyazdi

Received: 16 October 2024
Revised: 16 December 2024
Accepted: 19 December 2024
Published: 22 December 2024

1. Introduction

Water quality (WQ) provides valuable information related to the physical, chemical, and biological status of a water resource. It can be assessed in terms of different parameters quantifying the concentrations of certain organisms or chemical substances [1]. Surface water quality is affected by a range of anthropogenic and natural factors, including population growth and urbanization, which accelerates the rate at which untreated sewage and agricultural chemicals are discharged to natural bodies of water such as lakes [2,3].

Monitoring the water quality of these resources is critical for the sustainable management, protection, and conservation of the lake ecosystem.

The continuous deterioration of water quality globally, especially in regions like the Global South, poses a major threat to human health and other living organisms [2]. Improving water quality heavily relies on effective monitoring, but large data gaps often exist, particularly in southern regions [4]. Surface water quality monitoring helps address this by regularly measuring key parameters such as turbidity, temperature, and dissolved oxygen. However, in many cases, the data required to fully understand water quality trends is limited due to the costs, time, and labor required for traditional in situ monitoring.

Traditionally, in situ monitoring methods have been the primary approach to collecting water quality data. While these methods are effective and accurate, they face significant challenges. In situ water quality monitoring campaigns are often costly, time-consuming, laborious, and have limited spatial and temporal coverage. As a result, despite their accuracy, these challenges restrict the overall scope of water quality assessment, making it difficult to obtain comprehensive, real-time data across large or remote areas.

With advances in technology, remote sensing (RS) has emerged as a powerful tool for water quality monitoring. By using images taken by sensors, satellites, or drones, different information about the Earth's surface or any object on the surface can be derived [5]. This information is obtained by processing the measurements from the reflection and emission of radiation captured by a satellite's sensor from the surface of the Earth [6]. Due to the ease of data collection and its cost effectiveness, the utilization of remote sensing derived data has been increasing. Remote sensing can estimate key WQ parameters like chlorophyll-a, turbidity, and dissolved organic matter based on the water's optical properties. This ability to evaluate water quality over time with minimal physical effort presents a significant opportunity to improve water quality monitoring globally, especially in regions with large data gaps.

Different technologies and techniques have also been employed to advance water quality monitoring like the application of citizen science [7–9], unmanned aerial vehicle-assisted water quality measurement systems (UAMS) [10], fixed sensors measuring at certain frequencies utilizing the internet of things (IoT) for data transmission [11], and remote sensing, which is the focus of this study. Remote sensing allows water managers to evaluate the water quality of the whole water resource over time due to its greater spatial and temporal coverage [10].

Among the different types of remote sensing, optical remote sensing is used in retrieving water quality parameters. This takes advantage of already launched missions that are equipped with optical sensors. Using satellite imagery remotely sensed by optical sensors like Ocean and Land Colour Instrument (OLCI), or Moderate Resolution Imaging Spectroradiometer (MODIS) onboard satellites Sentinel-3 and Aqua/Terra, different water quality parameters can be estimated. Using the (1) empirical, (2) analytical, (3) semi-empirical, and (4) artificial intelligence (AI) retrieval modes on satellite (multispectral and hyperspectral) and non-satellite borne remote sensing data, water quality parameters such as chlorophyll-a (Chl-a), total suspended matter (TSM), dissolved organic matter (DOM), total nitrogen (TN), total phosphorus (TP), and chemical oxygen demand (COD) can be retrieved, some of which are optically active, while others can be derived using relationships with other substances or AI [12].

The potential of remote sensing for water quality monitoring is further demonstrated by studies such as those conducted by Huovinen et al. [13] and Nazirova et al. [14]. In 2019, a study was conducted by Huovinen et al. [13] to apply remote sensing in estimating key WQ parameters (lake surface water temperature (LSWT), turbidity, and chlorophyll-a) in Lake Panguipulli in Chile. In this study, they estimated the WQ parameters based on satellite images from Landsat 5, 7, and 8, and Sentinel 2 using ACOLITE software (version version 20180419.0 for Windows), which uses single algorithms for each of the parameters. In the case of turbidity, the semi-empirical algorithm of Dogliotti et al. was used, while the empirical Ocean Chlorophyll two-band (OC2v2) algorithm was used

to estimate chlorophyll-a. Huovinen et al.'s study showed accurate LSWT estimates, with good spatial and seasonal variation representation of the other parameters. On the other hand, high correlation was observed by Nazirova et al. [14] when comparing quasi-synchronous in situ data with RS data. Nazirova et al. [14] estimated turbidity and the suspended matter concentration from Landsat 8 and Sentinel 2 images using the algorithms of Dogliotti et al. and Nechad. Although Nazirova et al. [14] evaluated multiple retrieval algorithms, both studies applied single algorithms across the whole study area to estimate WQ parameters. This may have caused the inaccuracies in the observed results since doing so disregards the optical water type of the lake, which can also vary within a lake. As highlighted in a RS review by H. Yang et al. [12], the applicability of a retrieval algorithm is essential in making accurate estimates. In addition, they stated that this can be solved by using defined optical water types and the corresponding applicable retrieval algorithms. In this study, these were addressed by using global RS products that assign an estimation algorithm to each pixel of the satellite image of the lake depending on the identified optical water type of the pixel, ensuring a more accurate estimate.

Nowadays, various remote sensing products utilizing a combination of optimal algorithms can be found in open-source databases from different national space agencies, where they are usually characterized by spatial resolution, temporal resolution, and available variables. International institutions like the National Aeronautics and Space Administration (NASA) and European Space Agency (ESA) offer such products estimating water quality parameters using combinations of different algorithms. Prior to the release of these global remote sensing products, calibration and validation with in situ data is conducted, until a target accuracy is reached. Although these products estimate different parameters by adapting the optimal algorithms based on the inherent optical property (IOP) of a water body [12], there are still cases where low accuracy can occur, especially since calibration and validation is limited by the in situ data used. In this case, Nazirova et al. [14] noted that a lower correlation is to be expected; thus, regional retrieval algorithms are developed. Developing a regional retrieval algorithm is outside the scope of this study.

Global WQ RS products such as Copernicus Global Land Service (CGLS) and ESA Lakes CCI have been seeing increased use globally, like in the studies of Nkwasa et al. [15] and Nakkazi [16], which used these products in Lake Tana in Ethiopia and Lake Victoria in Tanzania, Uganda, and Kenya. The two studies showed that the two global WQ RS products show promising results for lakes in Africa, especially in terms of spatial and temporal variability. In Latin America, however, specifically for Lake Titicaca, documentation on the use of remote sensing products for water quality monitoring is rather scarce. One exception is a study by Baltodano et al. [17], which used Terrascope turbidity and chlorophyll-a products in the water quality analysis of Lake Titicaca. However, this study only focused on the Katari River Basin area of the lake. The inter-comparison of the applicability of these products for water quality monitoring of Lake Titicaca is not well studied. Thus, in this study, global remote sensing products estimating various water quality parameters were explored on the whole Lake Titicaca basin and compared with each other.

Increasing concern is seen towards the deteriorating water quality of Lake Titicaca [18]. With the current state of Lake Titicaca and its sheer scale, quicker and more cost-effective ways of water quality monitoring are necessary. To strengthen the water quality monitoring efforts for Lake Titicaca, this study explored global remote sensing products that estimate various water quality parameters. This was accomplished by (1) comparing two remote sensing derived water quality products while identifying the characteristics of the products; (2) validating remote sensing derived data with in situ water quality data, specifically LSWT and turbidity; and (3) illustrating and evaluating the spatiotemporal variability of LSWT, turbidity, and chlorophyll-a. The results of this study can aid the ministries of Bolivia and Peru in monitoring the lake water quality, and ultimately in decision making.

2. Materials and Methods

2.1. Case Study

Lake Titicaca is on the border of Bolivia and Peru. Located 3810 m above mean sea level with 8300 km^2 surface area, it is considered the highest lake among the world's large lakes, the largest lake in South America [19], and the most important water resource in the Andes [20]. Figure 1 shows a satellite image of the entirety of the lake, with Bolivia on the east and Peru on the west.

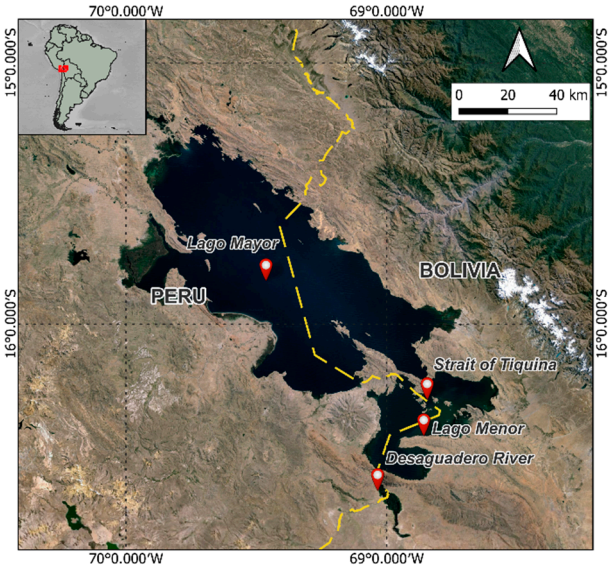

Figure 1. Lake Titicaca Landsat Satellite Image, 10 April 2013.

From the 57,500 km^2 catchment area, three-quarters is drained by six main rivers (Ramis, Ilave, Coata, Katari, Huancane, and Suchez) to the lake, which occupies 15% of the Lake Titicaca basin [21]. Having only one outlet from the lake, Desaguadero River, most of the water losses from the lake are through surface water evaporation [22]. This single outlet of the lake also contributes to the long water residence time of approximately 1300 years [23]. Lake Titicaca's basin can be categorized into the *lago* (lake), *pampa* (lake plain), *cerro* (lower hill slopes) at 3800 m to 4200 m altitude, and *puna* (high-altitude grasslands) at 4100 m to 4600 m altitude and above [24]. The *lago* portion of Lake Titicaca is further subdivided into Lago Mayor and Lago Menor (also called Lago Huiñaymarca), connected by the Strait of Tiquina. Lago Mayor is the larger part of Lake Titicaca with a surface area of 7131 km^2 and an average depth of 125 m, while Lago Menor covers 1428 km^2 and has an average depth of 9 m [25]. Lake Titicaca's catchment is characterized by two seasons, wet and dry, starting from December until March and April to November, respectively, January being the wettest month, and July the driest month [21,26].

For the population within the vicinity and neighboring areas of the lake, Titicaca is an important resource of water for domestic, agricultural, and industrial purposes [27,28]. Residents and indigenous people from both Bolivian and Peruvian sides of the lake depend on Titicaca for hunting, fisheries, aquaculture activities, and tourism [29,30]. Aside from sustenance, indigenous communities also consider Titicaca as a sacred lake where the deity Viracocha was said to have created the sun, the moon, and the stars [31]. Understanding the current state and maintaining good water quality is necessary to ensure that these ecological and sociocultural services are provided to the population and the local ecosystem that depend on this natural resource [32].

In the past, an oligotrophic state was observed across most of the whole lake, which was maintained in the deep areas of Lago Mayor until recent years; however, the shallow areas of Lago Mayor and Lago Menor have been transitioning into mesotrophic and eutrophic states, mainly due to the direct discharge of domestic waste into the lake, especially

from the northern villages of Lago Menor [33]. Cities like El Alto, southeast of Lago Menor, also contribute to the contamination of Lake Titicaca, specifically along Cohana Bay [32,33]. Aside from pollution caused by domestic wastes, heavy metals such as lead, copper, zinc, cadmium, and mercury have also been found to pollute the lake, some of which have a concentration exceeding international safety standards [34]. These metals can bioaccumulate in different organisms in the lake, especially fish, which are then consumed by the population. The increasing pollution levels in the lake have reached alarming levels, causing serious problems for residents and endemic species. In 2015, an algal bloom event occurred, caused by a longer rainy season, leading to the death of 10,000 endemic giant water frogs [33,35]. These studies show how quickly the water quality of Lake Titicaca is degrading. The limited WQ monitoring campaigns prove the difficulty of in situ monitoring. With the current state of Lake Titicaca and its sheer scale, quicker and more cost-effective ways of water quality monitoring are necessary, and this is where the knowledge of remote sensing comes into play, which was employed in this study.

2.2. Validation of Remote Sensing Data

Before global remote sensing WQ products are released, sufficient validation is conducted using a selected lake with ample monitoring data to ensure that the accuracy of the product reaches the target. Some of these lakes include Lake Huron and Lake Erie shared by the US and Canada, Lake Ijssel in the Netherlands, and Lake Taihu in China, among others, most of which are in the global north [36,37]. Since these products have global coverage and limited validation is conducted, consistent global accuracy is also expected to be limited. In this study, the accuracy of two global remote sensing WQ products, specifically LSWT and turbidity products, were validated with in situ derived WQ data in Lake Titicaca.

2.2.1. In Situ Data

In this study, in situ data were obtained through data requisition from government institutions of the two countries. In Peru, data were requested from the Autoridad Nacional del Agua (ANA). ANA is a government institution under the Ministry of Agrarian Development and Irrigation, which was established for the sustainable management and conservation of Peru's water resources [38]. Under ANA is the Proyecto Especial Binacional Lago Titicaca (PEBLT), which follows the vision of ANA and focuses on the binational water resource management of the Lake Titicaca basin. The data provided covers nine (9) monitoring campaigns from the years 2012 to 2020 (excluding 2014), comprising physicochemical, nutrients, and microbiological parameters for monitoring points across the whole lake extent. The data for the years 2012, 2013, and 2015 to 2020 consist of 24, 27, and 29 monitoring points, respectively. Since the data provided by PEBLT for the year 2012 did not have the coordinates of the monitoring points, it was not used in the analyses.

From Bolivia, water quality data for the years 2014, 2015, 2017, and 2018 was provided by the Unidad Operativa Boliviana de la Autoridad Binacional Autónoma del Sistema Hídrico TDPS (UOB-ALT-TDPS) under the Ministerio De Medio Ambiente y Agua (Ministry of Environment and Water) of Bolivia. The data from the Bolivian Ministry of Environment and Water also included physicochemical, nutrients, and microbiological parameters at monitoring points within the jurisdiction of Bolivia. In some cases where only the month and year of the monitoring campaign was stated for the in situ data obtained, it was assumed that the monitoring was performed during the 15th day of the month; doing so minimizes the difference between the assumed and the actual date of the monitoring. To lessen the bias caused by this assumption, two validations were performed: one validation utilizing in situ data from all campaigns, and one considering only in situ data from campaigns when sampling dates are certain. In total, in situ data from fourteen (14) monitoring campaigns were used in the validation, seven (7) of which have indicated dates for all monitoring points and seven (7) with assumed dates for the monitoring points. Appendix A provides an overview of the in situ data used in this study, while Figure 2 illustrates the

spatial distribution of the monitoring points in the lake and the corresponding frequency at which sampling was conducted at those points.

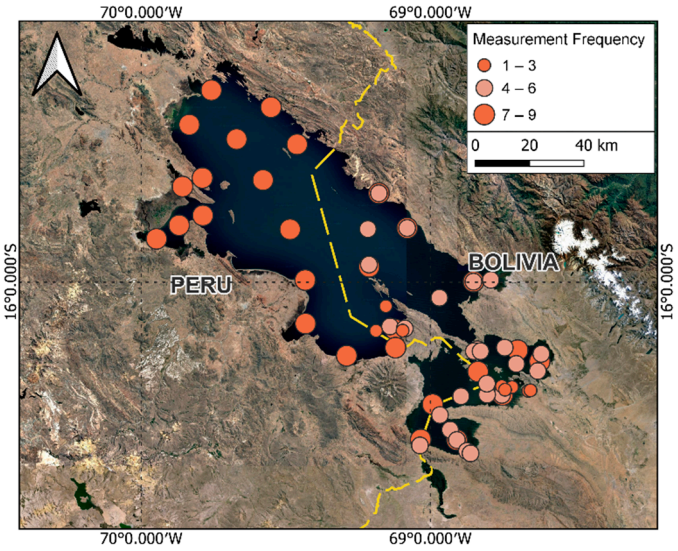

Figure 2. Measurement frequency of the monitoring points over Lake Titicaca across 14 monitoring campaigns.

Points measured between 7 to 9 times scattered over the whole lake are from the nine (9) PEBLT campaigns. Points measured once to 6 times are located on the Bolivian side of the lake. These are from the six (6) monitoring campaigns of UOB-ALT-TDPS.

2.2.2. Remote Sensing Products

Validation with in situ data was conducted with two (2) global products estimating water quality parameters: Copernicus Global Land Service (CGLS, https://land.copernicus.eu/en/products?tab=get_overview, accessed on 15 February 2024), now officially renamed Copernicus Land Monitoring Service or CLMS, and the European Space Agency Lakes Climate Change Initiative (ESA Lakes CCI, https://climate.esa.int/en/projects/lakes/, accessed on 17 August 2023). The period of data evaluation and comparison was from 2010 to 2020. Table 1 summarizes information of the two products such as coverage period, spatial resolution, satellite and sensors utilized, and the distributing agency for each database where water quality products were obtained. From these two databases, products were obtained for three water quality parameters, lake surface water temperature, turbidity, and chlorophyll-a concentration (trophic state index (TSI) in the CGLS database). Lake surface water temperature (LSWT) describes the amount of kinetic energy at the surface, about 0–1 m below the top surface of the lake [39,40]. LSWT is a Global Climate Observing System (GCOS) Essential Climate Variable (ECV), influencing the physical, biological, and chemical processes, which determines a lake's ecological status [41]. Turbidity is a measure of the reduction of light intensity passing through water due to different particles [42], while chlorophyll-a is a measurement indicating phytoplankton biomass, which can describe a water body's trophic status [43].

These parameters were retrieved using the different algorithms listed in Table 1 from data obtained from the satellite and sensor pair matched with the WQ parameter. To illustrate, the LSWT product from CGLS was obtained using the Optimal Estimation algorithm on L1b AATSR and SLSTR-A/B data, covering the periods 2002–2012 and 2016–present, respectively [44]. The CGLS Turbidity and Chlorophyll-a products were derived from L1b MERIS and OLCI data for the same two periods [45]. Both products follow the base methodology for LSWT retrieval. From the pre-processed satellite data, classification of lake water pixels that can be used for the LSWT retrieval is completed and the algorithm is then applied to retrieve LSWT before gridding the data and aggregating them temporally to

generate the product [44,46]. One distinct step in the ESA-CCI LSWT product development is determining the quality level of the retrieval, which is later used in the "collation" step in the processing [46]. ESA-CCI products are harmonized through daily collation by selecting pixels with the highest quality level and by applying per-lake inter-sensor adjustment factors based on a reference sensor [46]. WQ parameters based on lake water leaving reflectance (LWLR, turbidity and chlorophyll-a), are retrieved by the two products using the same processing chain, Calimnos. It starts with pre-processing including radiometric corrections, pixel identification, and atmospheric correction before classifying the optical water type (OWT) of each pixel, and then applying the specific algorithm for the OWT to retrieve the WQ parameters [45,46]. The estimation methodologies are further outlined in detail in the algorithm theoretical basis documents of the products.

Table 1. Summary of Relevant Information on the Remote Sensing Databases.

Database Name/Agency	Coverage Period and Temporal Resolution	WQ Product Spatial Resolution (m)	Satellite: Sensor	Retrieval Algorithm
Copernicus Global Land Service (CGLS)	May 2002 to present; 10-daily	100, 300, and 1000	Sentinel-3: SLSTR Envisat: AATSR [44]	LSWT: Optimal Estimation (OE) by MacCallum and Merchant (2012) [44]
			Sentinel-3: OLCI Envisat: MERIS [45]	Turbidity: Analytical algorithm of Binding et al. (2010), empirical algorithms of Vantrepotte et al. (2011), and Zhang et al. (2014). Algorithm parameters were empirically re-tuned by Neil et al. [45] Chlorophyll-a: OC2 algorithm, empirical band ratio of Gilerson et al. (2010), semi-analytical NIR-Red band algorithm of Gons et al. (2005), and adapted QAA algorithm of Mishra et al. (2014). Algorithm parameters were empirically re-tuned by Neil et al. [45]
European Space Agency (ESA) Lakes CCI	Sept 1992–2022; daily	1000	Envisat: AATSR Sentinel 3: SLSTR Metop: AVHRR Terra: MODIS [46]	LSWT: Optimal Estimation (OE) by MacCallum and Merchant (2012) [46]
			Envisat: MERIS Aqua: MODIS Sentinel 3: OLCI [46]	Turbidity: For MERIS data, similar algorithms were used as CGLS products. For MODIS data: empirical algorithms of Miller and Mckee (2004), Ondrusek et al. (2012), Chen et al. (2007), Petus et al. (2010), and Zhang et al. (2010) [46] Chlorophyll-a: For MERIS data, similar algorithms were used as CGLS products. For MODIS data: OC2, OC3, OC_HI, and empirical band ratio of Gilerson et al. (2010). Algorithms were re-tuned empirically by Neil et al. [46]

Global remote sensing water quality products offer different ways of obtaining data. The process of obtaining data for each of the two water quality products is outlined with the utmost detail.

Copernicus Global Land Service (CGLS)

Version 1 of the remote sensing water quality products offered by CGLS was downloaded via file transfer protocol (FTP) using the Filezilla client, with the FTP host: ftp.globalland.cls.fr, accessed on 15 February 2024. Appendix B shows the dataset and the corresponding paths in the FTP server. The first dataset is a 300 m resolution product

containing bands with information on mean turbidity and trophic state index, among other water quality parameters [47]. The second product specifically contains lake surface water temperature data at 1 km resolution [48]. For both datasets, two (2) time periods were considered when downloading the remote sensing data, the 1st of January 2010 to the 31st of December 2012, and the 20th of April 2016 to the 31st of December 2020. This was due to the unavailability of data from 2013 to the first few months of 2016 in the CGLS database. The downloaded data were in NetCDF format, containing 10-day aggregated estimates of the WQ parameters. The 10-day temporal aggregation of the LSWT product was based on a weighted average considering the weights assigned to the uncertainty of the observations, while the aggregation of the turbidity and TSI product was based on the lake surface reflectance that is the statistically most representative reflectance spectrum within the 10-day period [44,45]. Since each NetCDF file from CGLS has global coverage, each file was clipped to the extents of Lake Titicaca using a script in Python before the analysis.

ESA Lakes CCI (ESA-CCI)

ESA-CCI remote sensing water quality version 2.0.2 products were downloaded from the Centre for Environmental Data Analysis (CEDA) archive using the Lakes CCI Tools found on Github (https://github.com/cci-lakes/lakes_cci_tools, accessed on 17 August 2023) [49]. The tools include Python scripts, which were used to check the data availability for the lake and download data specifically for the lake. Downloading data using the Lakes CCI tools requires input such as the Lake ID (20 for Lake Titicaca), which was necessary for the script to mask the files and download data for the specific lake only. From this product, data for the period 1 January 2010 to 31 December 2020 was downloaded. Similar to the CGLS data, the files are in NetCDF format containing different data bands, each containing data for a specific water quality parameter, but with daily aggregation.

Although the two products have different temporal aggregations, the comparison was made without aggregating the ESA-CCI to 10 days since one of the aims of this study was to evaluate the products for water management as they are. Post-processing like aggregation can be considered, depending on the interests and needs of the water managers that will utilize the products.

As part of preprocessing, the downloaded NetCDF files from CGLS and ESA-CCI were converted to raster files separated into the parameters of interest (lake surface water temperature, turbidity, and chlorophyll-a concentration) for ease of processing. One of the water quality products of CGLS is the trophic state index (*TSI*), which is derived from the phytoplankton biomass by proxy of chlorophyll-a. Prior to the analysis, the trophic state index data was converted to chlorophyll-a concentrations using the rearranged *TSI* equation from Carlson [50], which was the basis of the conversion of chlorophyll-a to *TSI* in the CGLS product [45]:

$$Chla = e^{\left(\frac{2.04 - 6 \times \ln(2) + \frac{TSI \times \ln(2)}{10}}{0.68}\right)} \quad (1)$$

where *Chla* = the chlorophyll-a concentration, and *TSI* is the trophic state index.

2.2.3. Matching In Situ Data with RS Data

To create a comprehensive comparison of the water quality data, remote sensing data closest to the spatial and temporal location of the in situ measurement at the monitoring points were extracted for evaluation. Remote sensing data exactly at the sampling coordinates of the in situ data were extracted for the validation. The specific pixel from the products extracted at the in situ sampling point was considered to have sufficient quality to represent the WQ parameter at that point considering the temporal aggregation method employed for the CGLS products [44,45] and the harmonization technique of the ESA-CCI products [46] described in the previous section. A match-up window of ±3 days, consistent with other studies [13], was maintained as much as possible for the observations with available monitoring campaign dates. However, since the CGLS data has a 10-daily spatial resolution [44,45], some points have a match-up window exceeding the ±3 days match-up

window. The match-up window used in the validation ranges from ±1 day to ±18 days and 0 to ±9 days for CGLS and ESA-CCI, respectively. Both products were validated using the in situ data obtained from various monitoring campaigns over the lake.

2.2.4. Statistical Analysis

As a measure of the accuracy of the remote sensing derived water quality parameters, various statistical parameters such as coefficient of determination R^2, bias, Root Mean Square Error ($RMSE$), and combined error (E_{com}) were used. Due to the importance of both $RMSE$ and bias, Woo and Park [51] combined the two measures of error to E_{com}. The following equations define these statistical parameters:

$$R^2 = 1 - \frac{\sum(x_i - \hat{x}_i)^2}{\sum(x_i - \overline{x})^2} \quad (2)$$

$$Bias = \frac{1}{N}\sum_{i=1}^{N}(x_i - y_i) \quad (3)$$

$$RMSE = \left(\frac{1}{N}\sum_{i=1}^{N}(x_i - y_i)^2\right)^{1/2} \quad (4)$$

$$E_{com} = \left(RMSE^2 + Bias^2\right)^{1/2} \quad (5)$$

where x_i = the water quality parameter value obtained from remote sensing products, y_i = the in situ water quality parameter measurement, $\hat{x}_i$ = the predicted water quality parameter value based on the linear regression of remote sensing and in situ data, $\overline{x}$ = the mean of the remotely sensed parameter, and N is the number of the data points. An overall validation was conducted by comparing in situ data from all of the monitoring campaigns to the remote sensing data.

2.3. Spatiotemporal Analysis

To better understand the WQ dynamics of Lake Titicaca, spatiotemporal analysis was conducted for the three water quality parameters, LSWT, turbidity, and chlorophyll-a concentration. The spatial analysis provides an insight into the spatial patterns of the WQ parameters and the long-term monthly evolution of this pattern, while the temporal analysis illustrates seasonal patterns (either existent or not) and the trend of the parameters in time and the level of significance of this trend.

2.3.1. Spatial Analysis

Prior to the calculations, filtering of the raster files was completed and only raster files with more than 80% of pixels containing data for the whole lake were used to calculate the long-term monthly means. The percentage used is a balance of the adequacy of data for the calculation, ensuring that each month of the year has a representative map, and ample coverage of the lake surface area. After filtering, a buffer mask of one-pixel distance along the shorelines was applied to the raster files from the turbidity and chlorophyll-a products, following the recommendation from Simis et al. [45], to reduce the uncertainties caused by mixed land-water pixels along the shorelines and adjacency effects.

Using a Python script, the converted raster files from the preprocessing were read, filtered, and stored in data frames, which were stored in lists, in which one list element contains data for one month. Monthly means throughout the period of interest were then calculated and subsequently used to obtain long-term monthly means. The results of the calculation were saved as 12 separate raster files corresponding to each month of the year. After calculation of the long-term monthly means for the spatial analysis, the results were visualized side by side with the maps for each month, along with a color bar to represent the parameter values. Python version 3.9.13 was used for the spatial analysis and other

analyses in this study. The main Python packages used for this analysis are Rasterio [52] and numpy [53].

Using the 29 monitoring points from the PEBLT campaigns as a starting point, water quality hotspots (WQH) were identified from the long-term mean turbidity and chlorophyll-a estimates of the two products. The 29 monitoring points served as the starting point in the identification of hotspots due to their good spatial distribution in the lake, covering important areas. Identification of these WQHs was based on the long-term mean concentration of the WQ parameter for the study period 2010 to 2020 at the monitoring points in comparison with the WQ standards of Bolivia and Peru. Locations that have a long-term monthly mean concentration exceeding the WQ standards are considered as WQHs. Bolivia requires a turbidity below 50 NTU for Class C or general purpose waters, while Peru limits turbidity below 100 NTU for Subcategory B waters or recreational waters [54,55]. Of these 29 points, all were identified to be within the standard for lake surface water quality in terms of turbidity, having values below 10 NTU. Thus, based on turbidity, there are no WQHs. On the other hand, based on the eutrophication limits of 6.4 mg/m^3 chlorophyll-a concentration [50], thirteen (13) WQHs were identified. These hotspots, as shown in Figure 3, were the locations where temporal analysis was conducted. The coordinates of the hotspots are included in Appendix C.

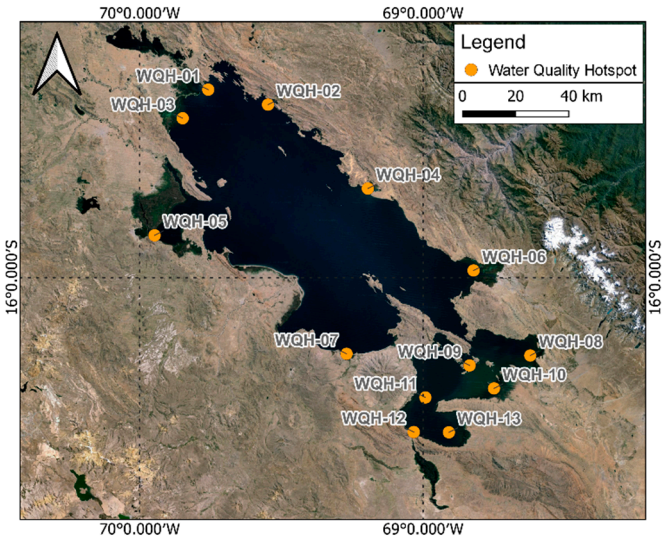

Figure 3. Identified Water Quality Hotspots in Lake Titicaca.

2.3.2. Temporal Analysis

As part of preprocessing for temporal analysis, a Python script loops through each raster file from the two remote sensing products to read and extract the water quality parameter value at the closest pixel for each water quality hotspot in Figure 3. This was performed for the periods mentioned in Section 2.2.2. The extracted WQ parameter values were stored in a csv file, along with the corresponding "Site ID" (or WQH) and "Date". The extracted data were sorted by hotspot and the time series for each WQ parameter was plotted.

To determine whether there is a significant temporal trend in the water quality of the lake, the Mann–Kendall (MK) test was conducted for the time series of the three parameters. Due to the seasonal nature of LSWT, the Seasonal MK test of Hirsch et al. [56] was applied to the parameter, while the Modified Mann–Kendall test using the Trend-free Pre-Whitening method as proposed by Yue and Wang [57] was applied to the two other parameters. Different studies show conflicting results on the seasonality of turbidity and chlorophyll-a [58,59], and in this study, it was observed that a seasonal pattern is not exhibited by the time series extracted for both WQ parameters. Mining activities and deforestation [17] affect the turbidity, while nutrient loading and turbidity [59] can affect the chlorophyll-a

concentration, which may not all strictly follow a seasonal pattern. Thus, the modified MK test was used for turbidity and chlorophyll-a. The MK test was applied using the pymannkendall [60] module in Python.

3. Results

3.1. Accuracy of the Remote Sensing Products

Tables 2 and 3 show the results of the validation of remote sensing derived data with in situ data for mean turbidity and LSWT, considering in situ data from all monitoring campaigns and considering only in situ data from campaigns with the indicated dates, respectively. Considering all in situ data, it can be observed in both products that there is an overestimation bias for lake surface temperatures, while there is an underestimation bias for mean turbidity measurements. In terms of the combined error (E_{com}) and correlation (R^2), both ESA-CCI products perform better. It should also be noted that for LSWT validation of ESA-CCI, remote sensing data were available for all 14 monitoring campaigns, while the other products, CGLS LSWT, CGLS and ESA-CCI turbidity, only have available data for eight monitoring campaigns from 2016 to 2020 for this first case.

Table 2. Summary of the Statistical Analysis for All Monitoring Campaigns for LSWT and Turbidity Considering All Monitoring Campaigns.

Variable	Product	R^2	Bias	RMSE	E_{com}	n	*p*-Value at 0.05 Alpha	Significance
LSWT	CGLS	0.296	0.408	1.817	1.862	143	2.25×10^{-12}	True
	ESA-CCI	0.326	0.206	1.635	1.648	312	2.31×10^{-28}	True
Turbidity	CGLS	0.036	−0.026	1.45	1.45	147	0.022	True
	ESA-CCI	0.061	−0.187	1.015	1.032	135	0.004	True

Table 3. Summary of the Statistical Analysis for All Monitoring Campaigns for LSWT and Turbidity Considering Monitoring Campaigns with Indicated Dates.

Variable	Product	R^2	Bias	RMSE	E_{com}	n	*p*-Value at 0.05 Alpha	Significance
LSWT	CGLS	0.005	1.835	2.636	3.212	28	0.715	False
	ESA-CCI	0.152	0.377	1.801	1.840	144	1.30×10^{-6}	True
Turbidity	CGLS	0.389	−0.465	1.137	1.228	30	2.30×10^{-4}	True
	ESA-CCI	0.061	−0.669	1.011	1.212	29	0.197	False

In the second case, it can be observed that the number of points used in the validation was greatly reduced due to filtering points without given dates. The same behavior was observed in terms of the biases of the two products in estimating the WQ parameters. However, a different observation can be seen in the correlation of the two products with the in situ turbidity data. With a significant correlation, CGLS performs better at estimating turbidity compared to ESA-CCI. Although there are differences in the results of the two cases, a low correlation is still present in both cases. The scatter plots showing the validation for each parameter and products are shown in Appendix D.

3.2. Long-Term Spatial and Monthly Pattern of Water Quality in Lake Titicaca

The spatial variation of the water quality parameters is visualized in Figures 4–6. Each figure shows the long-term average spatial pattern of the WQ parameters in separate maps for each month of a year. A color bar represents the values of the maps shown in the figures.

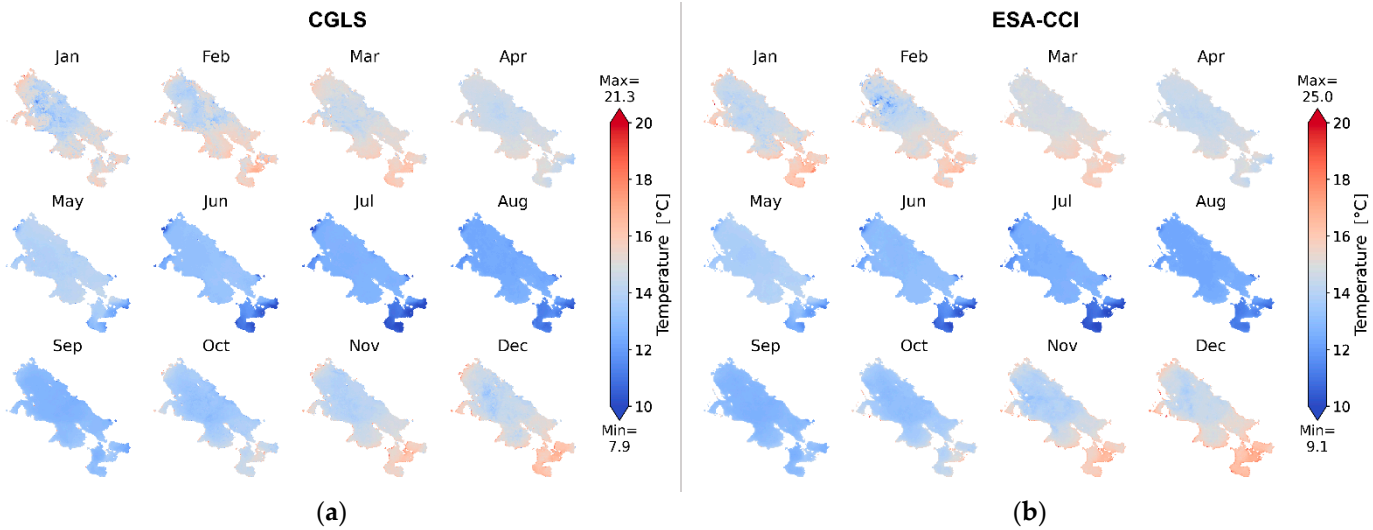

Figure 4. Long-term monthly mean LSWT maps for the period 2010–2020 for (**a**) CGLS and (**b**) ESA-CCI.

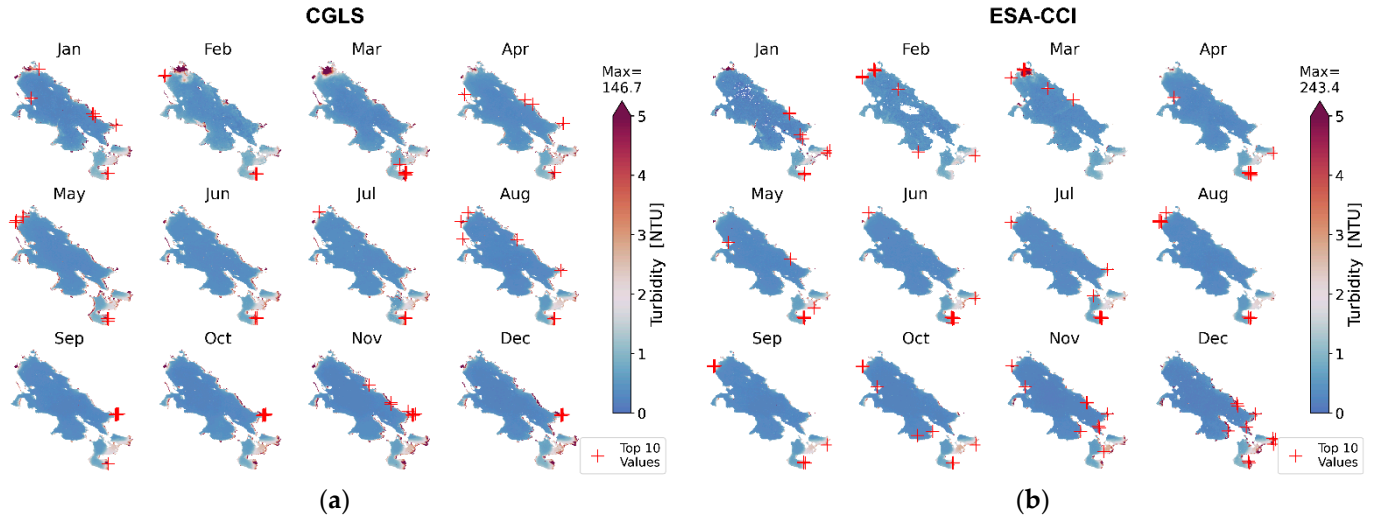

Figure 5. Long-term monthly mean turbidity maps for the period 2010–2020 for (**a**) CGLS and (**b**) ESA-CCI.

Across the whole lake, a well-mixed temperature can be observed. In terms of seasonal pattern, a consistency with the seasonal weather conditions is observed, with high temperatures from November to April, and low temperatures in the remaining months. The lowest temperatures can be observed in July and August, with lower temperatures occurring south of Lago Menor. During the warm months, the highest temperatures are observed in Lago Menor instead. The temperature difference between Lago Mayor and Lago Menor is caused by the significant difference in the depths of the two areas. Lago Menor, being shallower, has less heat capacity, and thus is more susceptible to rapid temperature changes compared to the deeper Lago Mayor [55]. Comparing the maps for mean lake surface water temperatures shows that the estimates from both products are almost identical with each other, spatially and seasonally.

Figure 5 shows that higher turbidity can be observed north of the lake and in the southern portion of Lago Menor. On average, there is high turbidity in the north of the lake, the outlet of the Ramis River, during the start of the year until the month of April. The turbidity north of the lake decreases while it increases in the southern half of Lago Menor. High turbidity can also be observed along the shores of the lake. In general, the inner parts

of the lake have lower turbidity. Spatially, a similar spatial and monthly pattern can be observed for the two turbidity products. However, the high turbidity along the shores is not as pronounced in the ESA-CCI estimates compared to the Copernicus GLS.

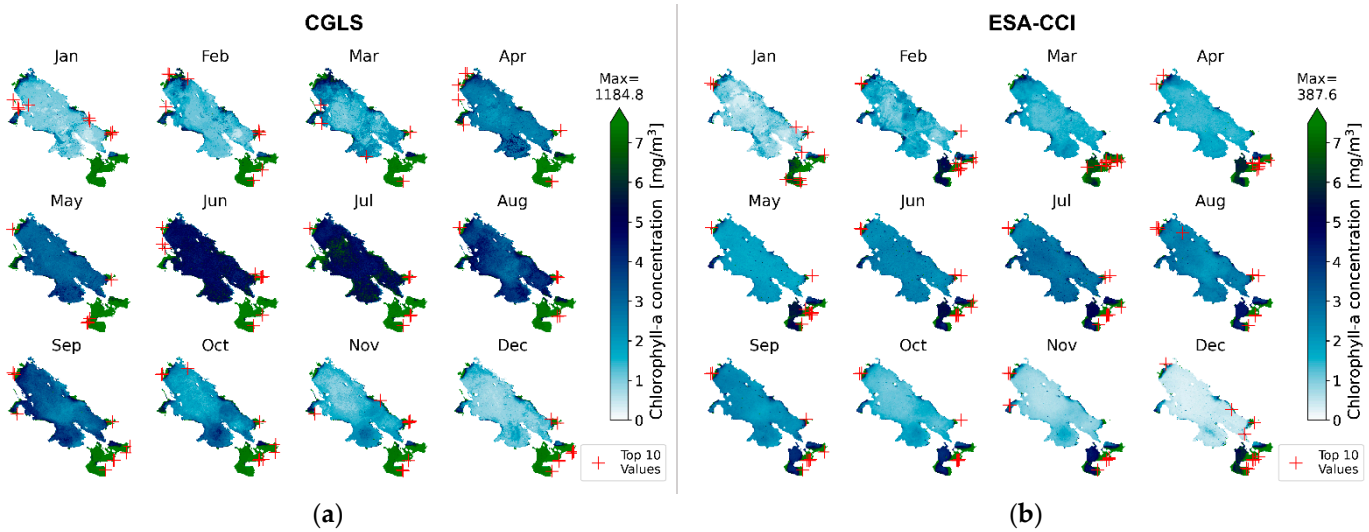

Figure 6. Long-term monthly mean chlorophyll-a concentration maps for the period 2010–2020 for (**a**) CGLS and (**b**) ESA-CCI.

The red crosses locate the ten (10) highest long-term monthly turbidity. Based on frequency, the critical point in Lago Menor is the Cohana Bay, the Katari River basin discharge region (near the Desaguadero river, south of the lake). In Lago Mayor, the critical points are the outlet of the Keka Achacachi river (SE Lake Titicaca) and near the district of Pusi (NW Lake Titicaca).

CGLS and ESA-CCI chlorophyll-a concentration estimates in Lake Titicaca are highest in Lago Menor and the bays in the east and northwest, where the bays of Ancoraimes city can be found and where the major rivers Suchez, Coata, Ramis, and Huancane terminate. The high concentration in Lago Menor is due to it being shallower, making it more susceptible to eutrophication caused by anthropogenic activities [61]. Concentrations in Lago Mayor are almost uniform except for the high concentrations along parts of the bays. The months of June and July have the highest concentration, while December and January have the lowest. ESA-CCI estimates show less pronounced high concentrations during the months of June and July and in Lago Menor, concentrations are not as uniform as the CGLS estimates.

There are two critical points identified in terms of chlorophyll-a concentrations, one for Lago Mayor and one for Lago Menor: the outlet of Keka Achacachi river (SE), and the outlet of Katari River, Cohana Bay (SE), respectively.

In the study period, estimates from both products show consistency with each other in terms of spatial patterns and magnitudes, with very few discrepancies. Table 4 shows the mean WQ parameter values over the whole study period for the two regions of the lake, Lago Mayor and Lago Menor. The mean values are calculated separately for the regions of the lake due to the significant differences of the parameter values, specifically for turbidity and chlorophyll-a, with Lago Menor being more contaminated. The two products estimated the average surface temperature of Lake Titicaca at approximately 14 °C, which is consistent with observations [62]. As observed in Figure 4, the surface water is warmer in Lago Menor during the warm months, which is also observed in the calculated long-term mean temperatures.

Table 4. Long-term mean water quality parameter estimates from the two products in each region of Lake Titicaca.

Product	Lake Region	LSWT	Turbidity	Chlorophyll-a
CGLS	Mayor	13.90	0.76	3.62
	Menor	13.93	1.92	16.36
ESA-CCI	Mayor	13.88	0.49	2.06
	Menor	14.04	1.49	10.94

3.3. Temporal Variability and Trends of Lake Titicaca Water Quality

Figures 7–9 show the time series of each water quality parameter (lake surface water temperature, turbidity, and chlorophyll-a concentration, respectively) with the estimates of the remote sensing products plotted on top of each other. Each subplot shows the temporal evolution of a parameter in a water quality hotspot.

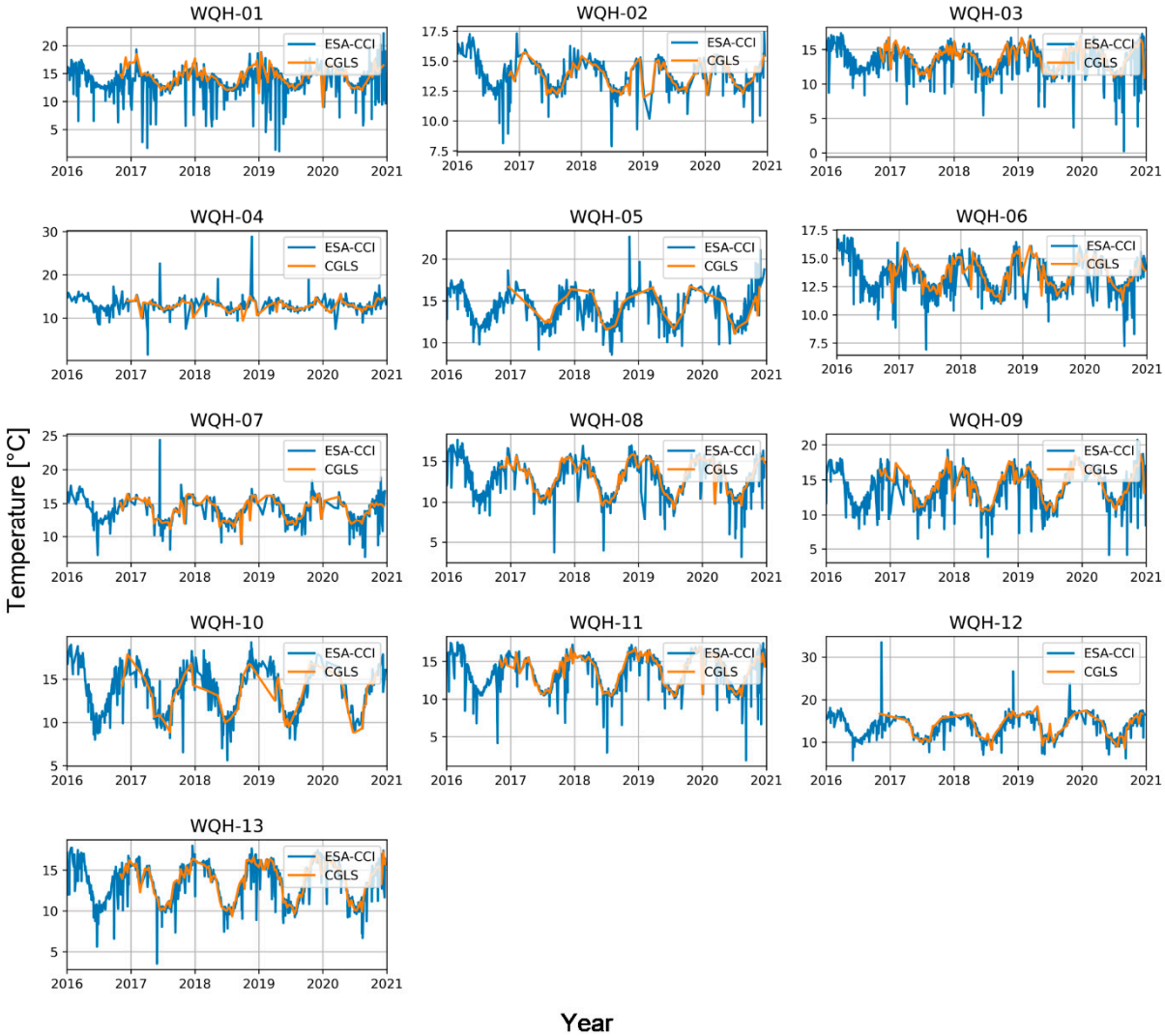

Figure 7. Temporal Pattern Comparison of Lake Surface Water Temperature (LSWT) for the Remote Sensing Products at Each Water Quality Hotspot (WQH).

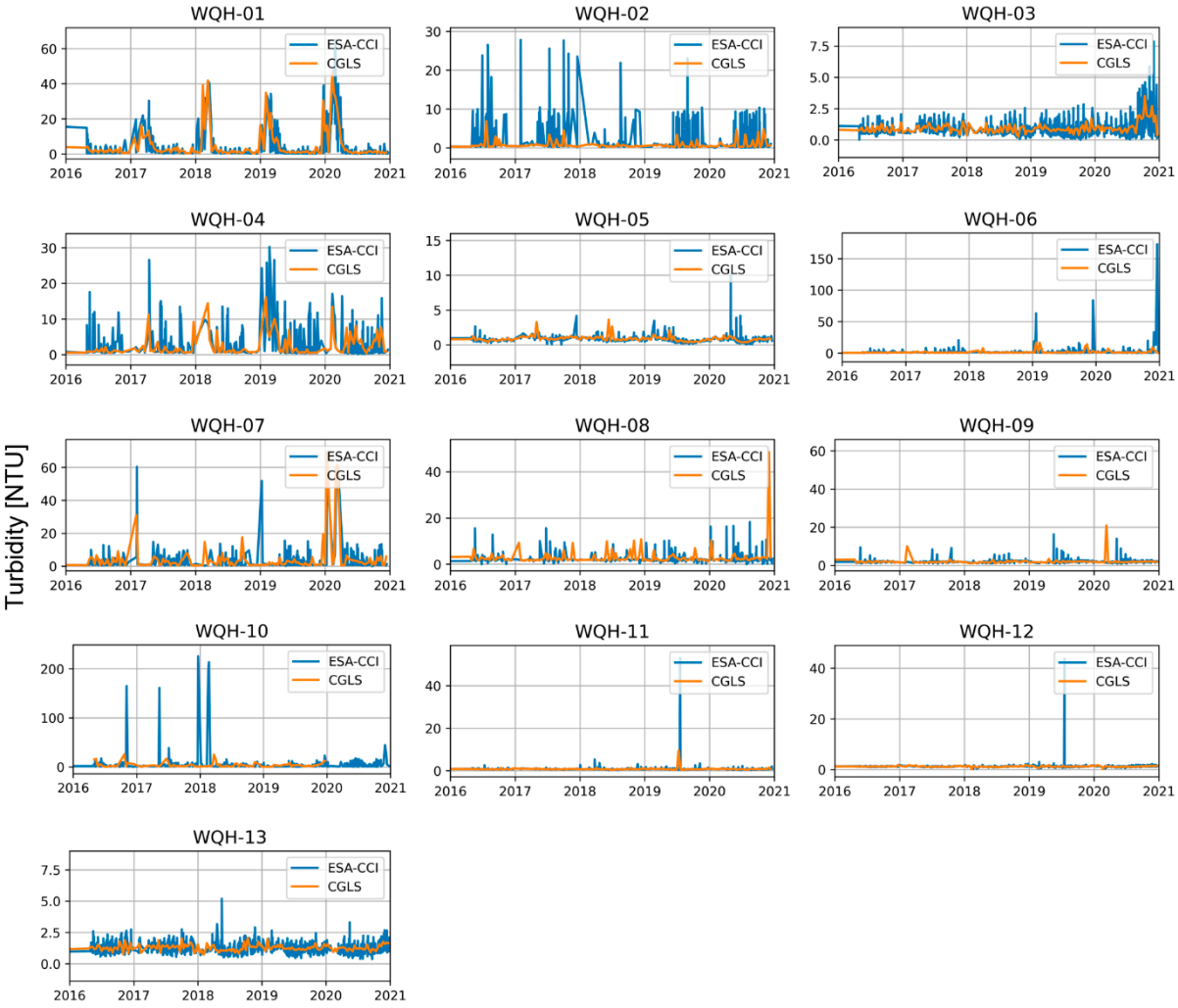

Figure 8. Temporal Pattern Comparison of Turbidity for the Remote Sensing Products at Each Water Quality Hotspot (WQH).

Temporally, the CGLS and ESA-CCI LSWT estimates are very consistent with each other, showing seasonal fluctuation of LSWT. The magnitude of the estimates is also consistent with each other, as shown by the almost perfectly overlapping plots, except for some extremes in the ESA-CCI estimates.

In terms of the mean turbidity temporal pattern, the seasonal variability is less apparent compared to LSWT. There is also less consistency with the estimates between the two products. A lot of high peak estimates are present in the ESA-CCI product, which are not present in the CGLS estimates.

The chlorophyll-a estimates show the least consistency between the two products and a seasonal pattern is not present in the time series of the estimates. More high peaks are also present in the ESA-CCI estimates. Using the Mann–Kendall test, the trends of the temporal pattern of the water quality parameters were determined. Figures 10–12 show the results of the Mann–Kendall test.

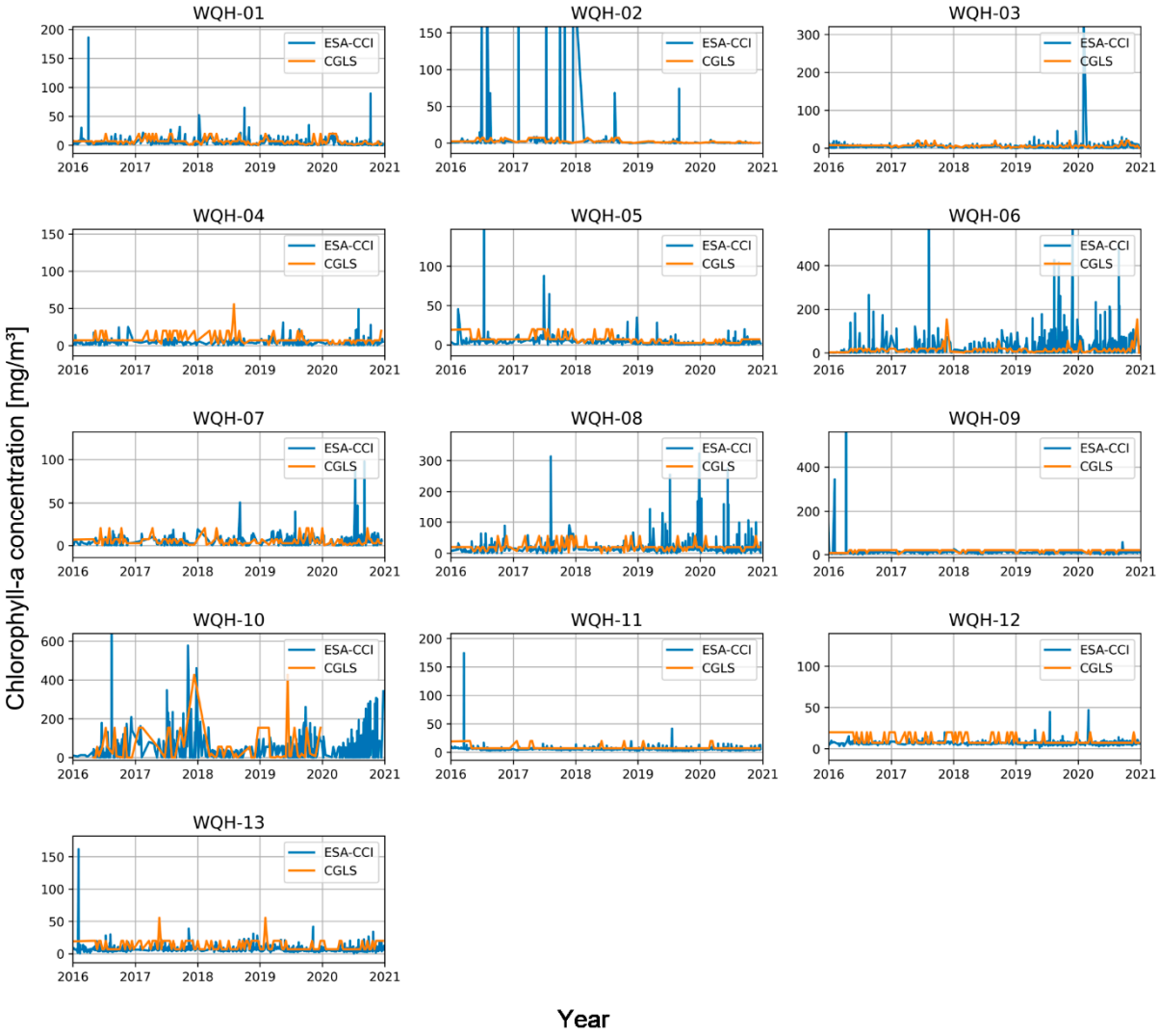

Figure 9. Temporal Pattern Comparison of Chlorophyll-a Concentration for the Remote Sensing Products at Each Water Quality Hotspot (WQH).

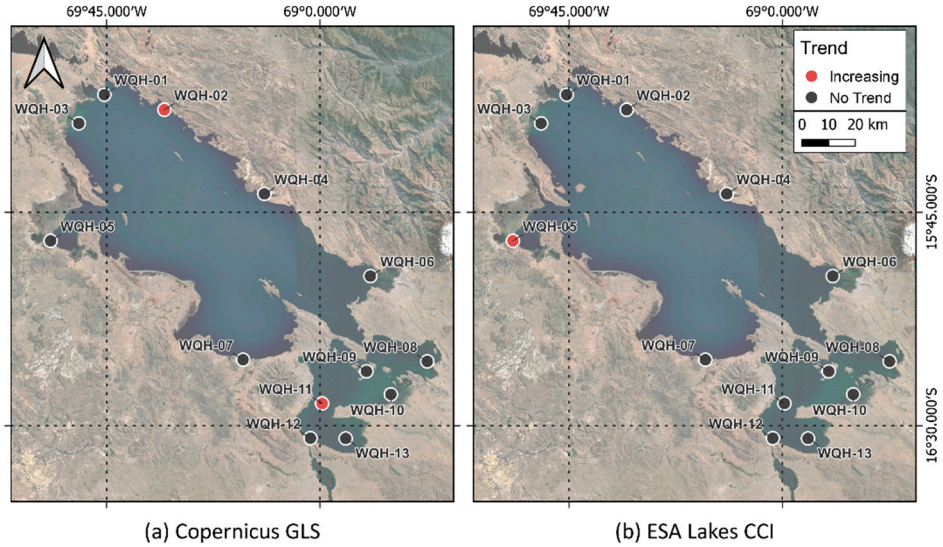

Figure 10. Mapped Mann–Kendall Test Results for Lake Surface Water Temperature.

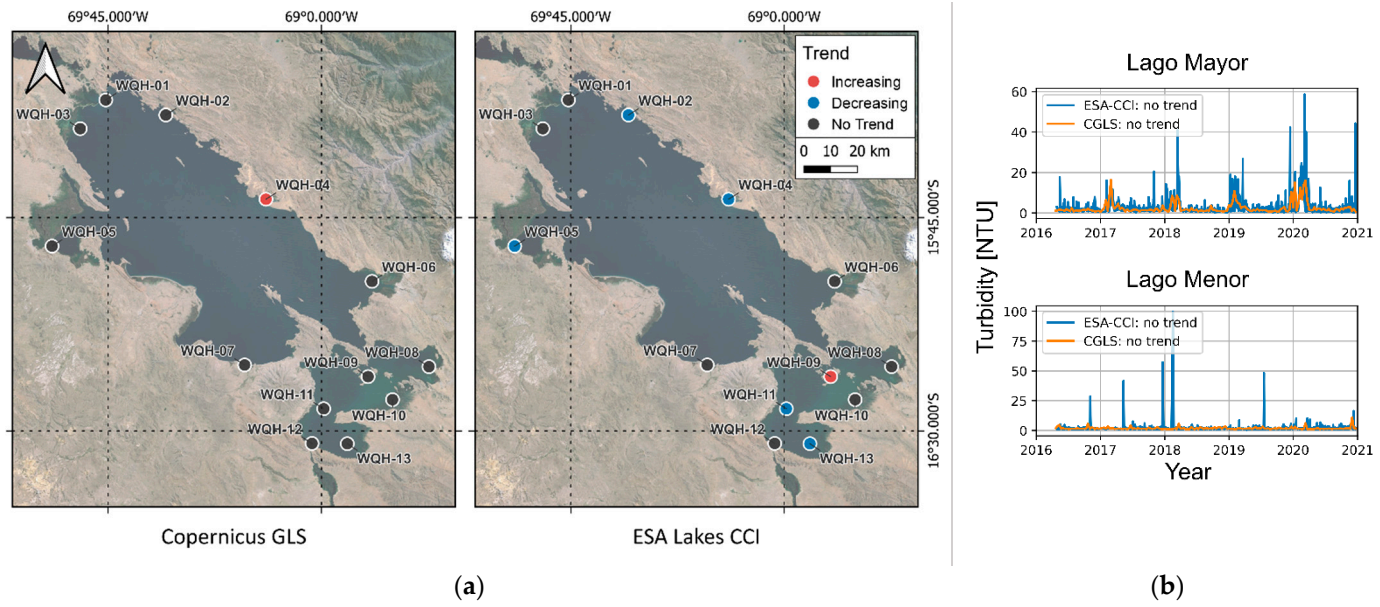

(**a**) (**b**)

Figure 11. (**a**) Mapped Mann–Kendall Test Results for Turbidity and (**b**) Lake Aggregated Time Series of the Turbidity Data Indicating the Calculated MK Trend.

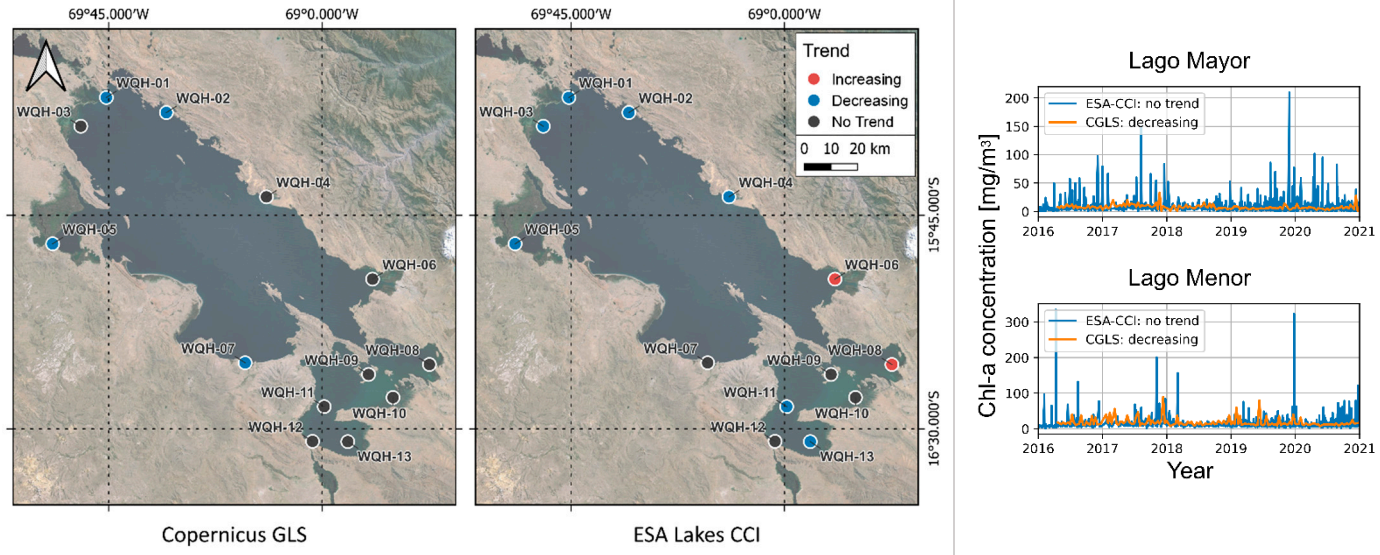

(**a**) (**b**)

Figure 12. (**a**) Mapped Mann–Kendall Test Results for Chlorophyll-a and (**b**) Lake Aggregated Time Series of the Chlorophyll-a Data Indicating the Calculated MK Trend.

Based on the results of the Mann–Kendall test for the LSWT time series of both products, the majority of the WQH have no trend, while only two and one WQH has an increasing trend for CGLS and ESA-CCI, respectively.

In terms of turbidity estimates, most WQH also have no temporal trend in the CGLS estimates, with only one point having an increasing trend. For the ESA-CCI estimates, the WQH are almost equally split between no trend and a decreasing trend, and similar to CGLS, only one point has an increasing trend. Aggregating the WQH time series per lake showed that most of the calculated trends for the WQHs exhibit a similar overall trend for Lago Mayor and Lago Menor. For both lakes, there seems to be no significant trend in the turbidity levels based on the two products.

Finally, chlorophyll-a concentration estimates show mostly decreasing trends from ESA-CCI, while CGLS shows mostly no trends followed by decreasing trends. Some points

with an increasing trend are also observed in the ESA-CCI estimates located at the outlets of Keka Achacachi and Katari River. Unlike turbidity, MK trends identified from each WQH do not agree with the trends of the aggregated time series. This is especially evident with the ESA-CCI trends in Lago Mayor, where chlorophyll-a is observed to be decreasing; however, when aggregated, the trend disappears.

4. Discussion

Two global remote sensing products estimating water quality parameters, Copernicus GLS and ESA Lakes CCI, were explored and evaluated for Lake Titicaca. Validation and comparisons were made between the in situ measurements and remote sensing derived LSWT and turbidity data over 14 monitoring campaigns using statistical analysis. The spatiotemporal variability of LSWT, turbidity, and chlorophyll-a from the two products was also analyzed and compared, through visual inspection and Mann–Kendall trend analysis.

4.1. Global Remote Sensing Water Quality Products Accuracy

The comparison of RS derived LSWT and turbidity data with the in situ data showed low accuracies in both products evaluated in both validations performed. One factor that may have caused the discrepancies is the measurement methodology employed during in situ campaigns, especially the depths at which water quality parameters are measured. The in situ data shows that measurements were mostly conducted at 20% and 80% depth of the lake at each monitoring point, where data measured at 20% depth (from 0.3 m to 54 m) were used as surface measurements. On the other hand, remote sensing products estimate WQ parameters using satellite imagery from various sources, which uses optical and thermal remote sensing to measure lake water leaving reflectance (LWLR) and brightness temperature in the topmost surface of the lake, respectively. Measured LWLR is used to estimate optically active parameters such as turbidity and chlorophyll-a, while brightness temperature is used to retrieve LSWT [46]. Another factor that may affect the accuracy of RS with in situ data is the synchronization of both data. Since in situ measurements were not carried out for this study, and only available historical data were used, perfect synchronization of the remote sensing derived data and in situ measurements cannot be achieved. It should also be noted that due to missing information in the data, like the exact date of some monitoring campaigns, assumptions were made that may affect the accuracy in the validation. On average, a match-up window of 4 days and 1 day was used for the CGLS and ESA-CCI products, respectively. The higher match-up window of the CGLS data is caused by the 10-daily temporal aggregation of data, compared to daily aggregation in ESA-CCI. The observed mean match-up window for CGLS is outside of the $\pm$3 days recommended match-up window according to Huovinen et al. [13]. In a study by Nazirova et al. [14], in situ measurements were conducted at a time when satellite images were also taken, synchronizing both measurements, which resulted in a good correlation between the in situ and remote sensing data. The results of this study are in agreement with Nazirova et al. [14], since it was observed that ESA-CCI products perform better due to its closer average match-up window. This shows that asynchrony between data results in a lower correlation.

Additionally, the different correlation of each product to in situ data may also be affected by the differences in the algorithms used (both atmospheric correction and parameter retrieval) in the products, temporal aggregation, as well as the spatial resolution of the products [16]. Spatial resolution of the products is dependent on the resolution of the source satellite imagery, which varies for each product. One important factor that may also affect the comparison, which may often be overlooked, is the quality of the in situ data. For large lakes like Lake Titicaca, in situ measurements may not always have the best quality, due to different factors like the lake's size, accessibility to the different parts of the lake, resource limitations, and its transboundary nature, which can hinder extensive and comprehensive sampling [63–65]. In most cases, in situ data are taken as absolute and are considered the correct data. However, this is not always the case. There

are various factors that may lead to poor quality in situ measurements, such as human error, instrument error, and unfavorable site conditions. The same is true in terms of remote sensing data, which can easily be affected by cloud cover, atmosphere, sun glint, adjacency effect, and calibration errors [66]. According to Simis et al. [46], the challenging part of estimating global water quality parameters using remote sensing is developing universally applicable algorithms for both atmospheric correction and parameter estimation, especially due to the highly variable nature of inland water bio-optical properties. The low accuracies observed from the two validations performed highlights the need for local algorithms for more accurate estimates.

Overall, a better correlation with in situ data was observed with LSWT products compared to turbidity products. This is consistent with other studies [13,67] showing good agreement between LSWT estimates using RS data and in situ measurements. This is due to the LSWT retrieval being based on physics, which stabilizes performance across space and time [44], whereas the WQ parameters based on LWLR are retrieved using analytical and (semi-)empirical relationships of variables [46].

Although better results were obtained in the validation of LSWT products, there are still uncertainties caused by quick temperature fluctuations common in surface waters at high altitudes, and the fact that the exact time of the day the in situ LSWT measurements were taken. Overall correlation coefficients (CGLS: 0.30; ESA-CCI: 0.33) also showed low correlation in the validation despite being better than the turbidity products validation. Better product performance can be achieved by improving data preprocessing (water/non-water pixel identification, optical water type definition and identification, etc.), atmospheric correction and retrieval algorithms [68]. As remote sensing product quality is dependent on the input data quality, proper selection of satellite imagery is necessary. Moreover, UAV imagery obtained from high-resolution sensors and in situ water surface reflectance measurements, which are not influenced by the atmosphere, can complement satellite imagery as input data to WQ retrieval algorithms [69].

4.2. Spatiotemporal Variability of Water Quality in Lake Titicaca

Analysis of the spatiotemporal variability of Lake Titicaca water quality exhibited both similar and differing patterns across the two products. It is noteworthy that LSWT estimates from both products showed identical spatiotemporal patterns, which may be due to utilizing the same optimal estimation (OE) algorithm of MacCallum and Merchant [70], as well as sharing some of the same sources of satellite images. The spatial LSWT pattern shows an almost well-mixed temperature across the whole lake except for the lower temperatures in Lago Menor during cool months and higher temperatures in Lago Menor during warm months. This is caused by Lago Menor being shallower compared to Lago Mayor. Meanwhile, the temporal variability of LSWT is dictated by the local climate pattern of the catchment.

Spatially, the same long-term pattern can be deduced from the turbidity estimates of both products; however, a lesser extent of high turbidity is shown by the ESA-CCI product, especially along the shores. Higher turbidity is estimated north of the lake during the first quarter of the year and south of the lake during the last quarter of the year. This roughly coincides with the wet season in the catchment, which means rainfall run-off transports sediments to the lake, causing high turbidity. A similar spatial pattern can be said for the chlorophyll-a estimates, which just have a more widespread high concentration over Lago Menor. This observation agrees with the results of Ruiz-Verdu et al. [71]. Throughout the year, Lago Menor is eutrophic, while Lago Mayor fluctuates between mesotrophic and oligotrophic states based on the classification of Carlson [50]. The high concentrations in the different parts of the lake are driven by phytoplankton bloom due to nutrient loading from the tributary rivers during wet periods [17,71]. This also explains the temporal pattern of turbidity and chlorophyll-a; however, it is less pronounced than the pattern observed with temperature.

Looking at the ten highest long-term monthly turbidity and chlorophyll-a revealed some critical points in Lake Titicaca, which include Cohana Bay. Baltodano [17] studied the Katari River Basin and calculated high NDVI values along Cohana Bay, which they attributed to the presence of aquatic vegetation and noted that it can also be due to eutrophication reported from in situ monitoring [72,73]. The spatial analysis also identified new critical points like the area near the district of Pusi and the outlet of Keka Achacachi river, which are not yet studied.

The similarities in spatial patterns can be attributed to both products using the same processing chain, Calimnos, while the differences may have been derived from various factors. This includes differences in spatial resolution and temporal aggregation of 10-daily versus daily aggregation. The difference in the extent of high turbidity observations may be rooted in the inaccuracy of pixel identification along the shores of the lakes, and the adjacency effect from land pixels, which may have been aggravated by the spatial resolution. This was to be expected since improvements in the pixel identification algorithms were still being developed when the products were made; thus, assumptions were made that the Idepix module that identifies water pixels can adequately differentiate water pixels from mixed land/water pixels [45,46]. As highlighted by Stelzer et al. [74], a crucial step in the retrieval is assigning an optical water type to each pixel of a satellite image, which is heavily dependent on the identification of the pixel as water and the atmospheric correction. Thus, they recommended users mask a buffer of one pixel in the shorelines of the lake since it is difficult to control and flag the misidentification in the area, especially for users that are interested in lake averages rather than maps, to reduce errors and uncertainties of estimates near the shorelines [45]. This has been improved in the newer version of Calimnos used by the newest ESA-CCI products, which introduced mixed-water types to consider the effect of adjacent lands to water [46].

The temporal pattern of chlorophyll-a shows noticeable differences between products caused by the conversion from the trophic state index to the chlorophyll-a concentration as also explained by Nakkazi [16] and Baltodano [75]. This causes higher concentration peaks in the ESA-CCI estimates to be underestimated by the CGLS product due to the maximum value limit corresponding to a TSI of 100 in the algorithm used to convert TSI to chlorophyll-a concentrations. The observed data gaps, particularly for the period of 2013 to 2016, especially for the CGLS products, which were not included in the analysis, may be due to the scarcity of input data from satellite imagery.

Temporal trends of the WQ parameters at the WQHs are not in agreement with each other between the products, which is especially noticeable in the turbidity estimates, where no trends were mostly determined in CGLS, while a mix of trends were found for ESA-CCI. Aguilar-Lome et al. [76] found that there was an increasing trend in the LSWT of Lake Titicaca, which they attributed to the significant increasing trend of local air temperature. A study showed that there is an increasing trend in the turbidity of Lake Titicaca's waters. In contrast, chlorophyll-a trends across the whole lake were mostly consistent with each other, with a decreasing trend. Upon aggregating the turbidity and chlorophyll-a time series per lake, the calculated trends weakened, especially for the ESA-CCI estimates; thus, no significant trends were identified. This can also mean that the contamination is rather concentrated in some areas and does not affect the whole lake. Studies [33,77] also showed that increasing eutrophication is observed in the lake. In more turbid waters like the Lago Menor of Lake Titicaca, less light penetrates, thus hindering growth of aquatic plants, and in turn impacting chlorophyll-a. This shows how complex chlorophyll-a trend studies are, due to its highly susceptibility to uncertainties caused by the complexity of phytoplankton dynamics [78]. Another observation in this study is the high variability in the time series, especially with the ESA-CCI estimates. This high variability adds another complexity to trend analyses, which may obscure and weaken a trend [79]. Although trend analysis provides important information on the rate and trend of the change in the water quality of a lake, it does not provide an insight into the causes of this trend [79]. To shed light on the

causes of these trends, it is recommended to relate the drivers that may affect water quality trends, which can be achieved through land use and land cover change analysis.

4.3. Comparison of CGLS and ESA-CCI Products

Comparing the two global remote sensing WQ products in terms of temporal availability and resolution, WQ parameter availability, and estimate accuracy shows that both products have their advantages and disadvantages, depending on the focus of the application. One downside of the CGLS data is the 10-daily aggregation; however, it is available until the present. In contrast, the daily aggregation of ESA-CCI products is an advantage but the latest dataset, v2.1, only has data availability until the end of 2022. The ESA-CCI v2.1 dataset was released under the second phase of the project, which started in 2022 and is expected to last for three years. The finer spatial resolution of LWLR derived CGLS products gives it an edge over the 1 km resolution of ESA-CCI products. LSWT products, on the other hand, are just on par with each other when it comes to spatial resolution, accuracy of estimates and spatiotemporal variability. The same is true for the availability of WQ parameters; however, TSI estimates may not be as reliable when converted to chlorophyll-a and compared to the ESA-CCI product due to the limitations caused by the conversion algorithm. When it comes to spatial variability and estimate accuracy, ESA-CCI turbidity estimates are more dependable, especially along the shores due to the added mixed-water types in the Calimnos v2.1.

5. Conclusions

In this study, the feasibility of global remote sensing products for monitoring the water quality of Lake Titicaca was evaluated through a comparison with in situ measurements and an analysis of the spatiotemporal variability of LSWT, turbidity, and chlorophyll-a.

Validation of remote sensing derived data showed that LSWT estimates are better correlated with in situ data than turbidity estimates. On average, LSWT estimates have an overestimation bias, while the opposite is true for turbidity estimates. Inaccuracies are attributable to various factors such as measurement uncertainties, synchronization of data, atmospheric correction, the retrieval algorithms, and the spatial resolution. The observed spatial patterns from the three WQ parameters evaluated are accurate as verified by the actual field conditions and comparisons between each other, where high turbidity and chlorophyll-a are observed in Lago Menor and at the outlets of major tributaries. The consistency of the spatiotemporal and long-term monthly variability of LSWT between the two products is remarkable, which is due to the use of the same retrieval algorithm. In contrast, the difficulty in pixel identification, specifically along the shoreline, caused some minor differences in the estimated spatial variability of turbidity and chlorophyll-a. Temporally, only a few WQHs exhibited similar patterns for turbidity, even less for chlorophyll-a. This is due to the limitations caused by the conversion of TSI to chlorophyll-a concentration. Moreover, temporal trends of the WQ parameters were mostly not in agreement with each other. The decreasing trend mostly observed with chlorophyll-a estimates may be caused by the phytoplankton dynamics complexity.

The effects of the difference in the temporal aggregation of the two products are most evident in the temporal analysis, where a lot of peak highs and lows were observed in the ESA-CCI estimates, while the CGLS estimates do not exhibit these peaks. The difference between the temporal aggregations was retained during the analysis since one of the aims of this study was to evaluate the two products as they are. Further processing of data from the products is at the water managers' discretion as they see fit for their use case.

In terms of reliability, it can be said that the products are on par with each other, each with upsides and downsides. CGLS products are advantageous in the sense that they are available until the present, also given that the LSWT estimates yielded a higher accuracy. However, LWLR products (turbidity, chlorophyll-a) of ESA-CCI will be more reliable for spatiotemporal variability studies due to its more updated retrieval processing chain.

This study showed that water quality monitoring in Lake Titicaca using remote sensing products is possible, but it is not without its limitations. First, only two products were evaluated within a limited period restricted by the temporal availability of data. In future studies, it will be relevant to explore how the two products will compare with others, such as Terrascope, Ocean Color, NOAA Gap-filled products, and in the far future, data obtained from the recently launched PACE mission of NASA. In situ validation could also have been improved by conducting seasonal validation, which was not possible due to the availability of in situ measurements. Moreover, as rainfall greatly influences water quality dynamics [80], the effects of precipitation on the water quality of Lake Titicaca can also be evaluated. Lastly, trend analysis by itself does not provide insight into the causes of water quality degradation; thus, land use and land cover change analysis is recommended to relate drivers that may affect water quality in Lake Titicaca.

Overall, global remote sensing water quality products can be used to monitor Lake Titicaca, currently with limited accuracy. The accuracy can be improved with improved pixel identification, accurate optical water type definition, and better algorithms. This also highlights and supports Simis' [46] statement on the challenges of estimating global water quality parameters due to the highly variable bio-optical properties of inland waters. Thus, improvement of global WQ products is necessary to fit local conditions in tropical lakes to make the products useful for decision-making at the appropriate scale.

Author Contributions: Conceptualization, V.H.M., A.B. and A.v.G.; Methodology, V.H.M. and A.B.; Analysis, V.H.M. and A.B.; Resources, V.H.M., A.B. and A.A.; Writing—original draft preparation, V.H.M., A.B. and A.A.; Writing—review and editing, V.H.M., A.B., A.A. and A.v.G.; Supervision, A.v.G. All authors have read and agreed to the published version of the manuscript.

Funding: This research was supported by the Open Water Network: impacts of global change on water quality (project code G0ADS24N) and the AXA Research Chair fund on Water Quality and Global change.

Data Availability Statement: Dataset supporting the reported results of the study are available on request from the corresponding author.

Conflicts of Interest: The authors declare no conflicts of interest.

Appendix A

Table A1. Summary of In Situ Data Obtained and its Sources.

Campaign Date	Coverage	Parameters	Data Source	Monitoring Dates
Sept 2013	Whole lake	Turbidity, Temperature	PEBLT	Assumed
Oct 2013	Whole lake		PEBLT	Assumed
Mar 2014	Bolivia		IBTEN—ALT—UOB	Indicated
Oct 2014	Bolivia		IBTEN—ALT—UOB	Indicated
Sept 2015	Whole lake	Temperature turbidity, Temperature	PEBLT	Indicated
Oct 2015	Bolivia		IBTEN—ALT—UOB	Indicated
Apr 2016	Whole lake	Temperature	PEBLT	Indicated
Jun 2017	Whole lake	Turbidity, temperature	PEBLT	Assumed
Nov 2017	Bolivia		IBTEN—ALT—UOB	Assumed
Jul 2018	Bolivia		IBTEN—ALT—UOB	Assumed
Nov 2018	Whole lake		PEBLT	Assumed
Aug 2019	Whole lake		PEBLT	Assumed
Dec 2019	Whole lake		PEBLT	Indicated
Oct 2020	Whole lake		PEBLT	Indicated

Appendix B

Table A2. Summary of CGLS Dataset Used.

Dataset	FTP Folder Path	Parameters Included
300 m resolution, near-real time (nrt) based on Sentinel-3 and reprocessed based on Envisat	(2010–2012):/home/glbland_ftp/Core/BROCKMANN/dataset-brockmann-lwq-nrt-300m (2016–2023): /home/glbland_ftp/Core/BROCKMANN/dataset-brockmann-lwq-reproc-300m	Mean turbidity, Trophic state index
1 km resolution, near-real time (nrt) based on Sentinel-3 and reprocessed based on Envisat	(2010–2012):/home/glbland_ftp/Core/BROCKMANN/dataset-brockmann-lswt-nrt (2016–2023):/home/glbland_ftp/Core/BROCKMANN/dataset-brockmann-lswt-reproc	Lake Surface Water Temperature

Appendix C

Table A3. Identified Water Quality Hotspot Coordinates.

Hotspot Number	Latitude (°)	Longitude (°)
WQH-01	−15.336	−69.758
WQH-02	−15.389	−69.547
WQH-03	−15.437	−69.848
WQH-04	−15.685	−69.195
WQH-05	−15.85	−69.947
WQH-06	−15.974	−68.822
WQH-07	−16.268	−69.27
WQH-08	−16.274	−68.622
WQH-09	−16.309	−68.836
WQH-10	−16.39	−68.75
WQH-11	−16.422	−68.992
WQH-12	−16.544	−69.033
WQH-13	−16.545	−68.909

Appendix D

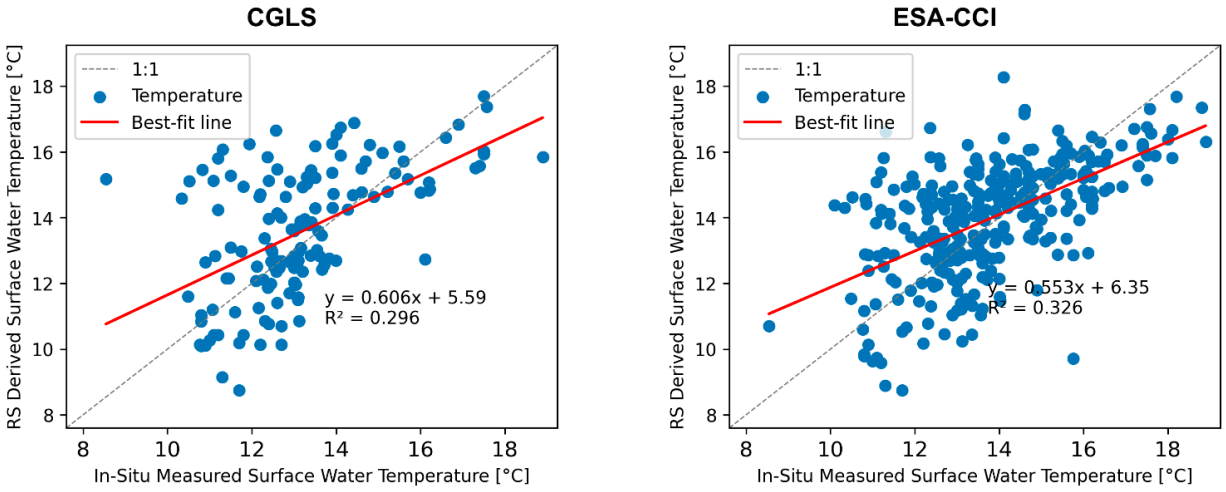

(**a**) (**b**)

Figure A1. Scatterplot of RS, derived vs. in situ measured, LSWT for (**a**) CGLS and (**b**) ESA-CCI, considering all monitoring campaigns.

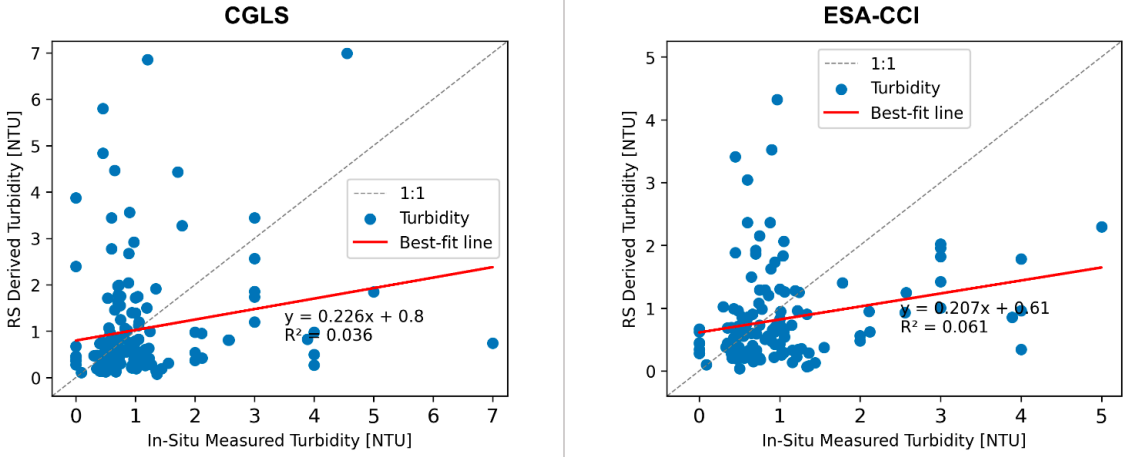

(**a**) (**b**)

Figure A2. Scatterplot of RS, derived vs. in situ measured, turbidity for (**a**) CGLS and (**b**) ESA-CCI, considering all monitoring campaigns.

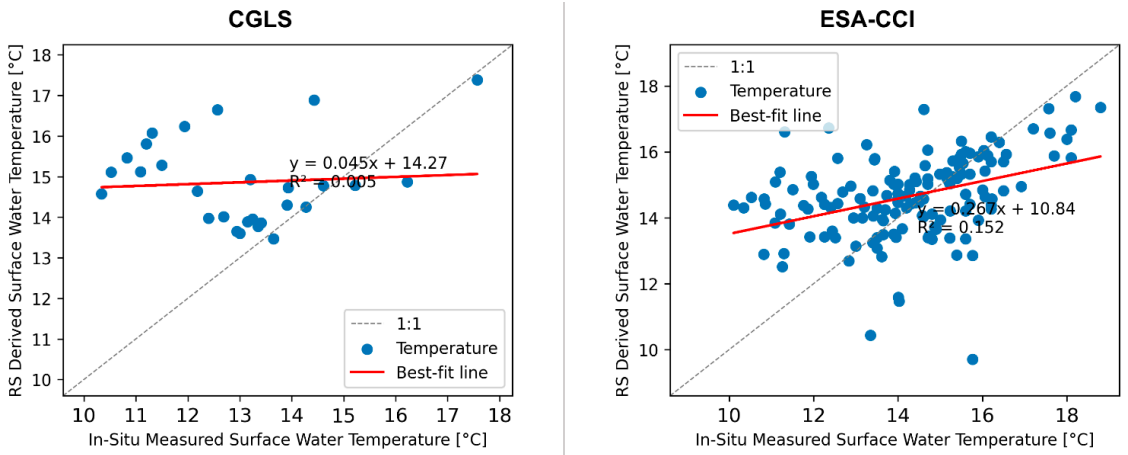

(**a**) (**b**)

Figure A3. Scatterplot of RS, derived vs. in situ measured, LSWT for (**a**) CGLS and (**b**) ESA-CCI, considering only monitoring campaigns with the indicated dates.

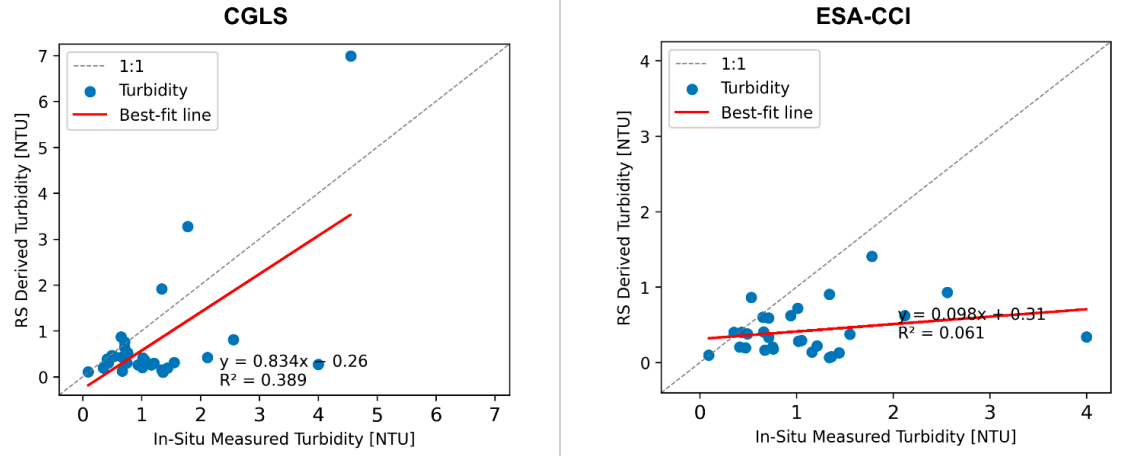

(**a**) (**b**)

Figure A4. Scatterplot of RS, derived vs. in situ measured, turbidity for (**a**) CGLS and (**b**) ESA-CCI, considering only monitoring campaigns with the indicated dates.

References

1. Da Silva, M.C.; Barbosa, A.E.; Rocha, J.S.; Fortunato, A.B. State-Of-The-Art For Surface Water Quality Modelling. In *State-of-the-Art Report on Quality Assurance in Modelling Related to River Basin Management*; Refsgaard, J.C., Ed.; HarmoniQuA projektet (EU-RTD projekt): Copenhagen, Denmark, 2002; Chapter 8; pp. 1–46.
2. du Plessis, A. Persistent Degradation: Global Water Quality Challenges and Required Actions. *One Earth* **2022**, *5*, 129–131. [CrossRef]
3. Bhateria, R.; Jain, D. Water Quality Assessment of Lake Water: A Review. *Sustain. Water Resour. Manag.* **2016**, *2*, 161–173. [CrossRef]
4. Warner, S.; Elsler, M.; Christ, K. Progress on Ambient Water Quality—2024 Update. Available online: https://www.unwater.org/publications/progress-ambient-water-quality-2024-update (accessed on 8 October 2024).
5. Read, J.; Torrado, M. Remote Sensing. In *International Encyclopedia of Human Geography*; Elsevier: Amsterdam, The Netherlands, 2009; pp. 335–346. [CrossRef]
6. USGS. *What Is Remote Sensing and What Is It Used for?* U.S. Geological Survey: Reston, VA, USA, 2024.
7. Hegarty, S.; Hayes, A.; Regan, F.; Bishop, I.; Clinton, R. Using Citizen Science to Understand River Water Quality While Filling Data Gaps to Meet United Nations Sustainable Development Goal 6 Objectives. *Sci. Total Environ.* **2021**, *783*, 146953. [CrossRef] [PubMed]
8. San Llorente Capdevila, A.; Kokimova, A.; Sinha Ray, S.; Avellán, T.; Kim, J.; Kirschke, S. Success Factors for Citizen Science Projects in Water Quality Monitoring. *Sci. Total Environ.* **2020**, *728*, 137843. [CrossRef] [PubMed]
9. Baltodano, A.; Agramont, A.; van Griensven, A. Combining Remote Sensing and Citizen Science to Bridge the Water Quality Data Gap: Lake Titicaca Case Study. In Proceedings of the IGARSS 2024—2024 IEEE International Geoscience and Remote Sensing Symposium, Athens, Greece, 7–12 July 2024; pp. 3621–3625.
10. Koparan, C.; Koc, A.B.; Privette, C.V.; Sawyer, C.B. In Situ Water Quality Measurements Using an Unmanned Aerial Vehicle (UAV) System. *Water* **2018**, *10*, 264. [CrossRef]
11. Mutri, M.A.; Saputra, A.R.A.; Alinursafa, I.; Ahmed, A.N.; Yafouz, A.; El-Shafie, A. Smart System for Water Quality Monitoring Utilizing Long-Range-Based Internet of Things. *Appl. Water Sci.* **2024**, *14*, 69. [CrossRef]
12. Yang, H.; Kong, J.; Hu, H.; Du, Y.; Gao, M.; Chen, F. A Review of Remote Sensing for Water Quality Retrieval: Progress and Challenges. *Remote Sens.* **2022**, *14*, 1770. [CrossRef]
13. Huovinen, P.; Ramírez, J.; Caputo, L.; Gómez, I. Mapping of Spatial and Temporal Variation of Water Characteristics through Satellite Remote Sensing in Lake Panguipulli, Chile. *Sci. Total Environ.* **2019**, *679*, 196–208. [CrossRef]
14. Nazirova, K.; Alferyeva, Y.; Lavrova, O.; Shur, Y.; Soloviev, D.; Bocharova, T.; Strochkov, A. Comparison of in Situ and Remote-Sensing Methods to Determine Turbidity and Concentration of Suspended Matter in the Estuary Zone of the Mzymta River, Black Sea. *Remote Sens.* **2021**, *13*, 143. [CrossRef]
15. Nkwasa, A.; Getachew, R.E.; Lekarkar, K.; Yimer, E.A.; Martínez, A.B.; Tang, T.; van Griensven, A. Can Turbidity Data from Remote Sensing Explain Modelled Spatial and Temporal Sediment Loading Patterns? An Application in the Lake Tana Basin. *Environ. Model. Assess.* **2024**, *29*, 871–882. [CrossRef]
16. Nakkazi, M.T.; Nkwasa, A.; Martínez, A.B.; van Griensven, A. Linking Land Use and Precipitation Changes to Water Quality Changes in Lake Victoria Using Earth Observation Data. *Environ. Monit. Assess.* **2024**, *196*, 1104. [CrossRef]
17. Baltodano, A.; Agramont, A.; Reusen, I.; van Griensven, A. Land Cover Change and Water Quality: How Remote Sensing Can Help Understand Driver–Impact Relations in the Lake Titicaca Basin. *Water* **2022**, *14*, 1021. [CrossRef]
18. New York Post Pollution Has Turned Sacred Lake Titicaca into a Toxic Cesspool. Available online: https://nypost.com/2017/03/02/pollution-has-turned-sacred-lake-titicaca-into-a-toxic-cesspool/ (accessed on 2 April 2024).
19. UNESCO. *Lake Titicaca*; UNESCO World Heritage Centre: Paris, France, 2005.
20. Agramont Akiyama, A.; Peres-Cajías, G.; Villafuerte Philippsborn, L.; Van Cauwenbergh, N.; Craps, M.; van Griensven, A. Framing Water Policies: A Transdisciplinary Study of Collaborative Governance; the Katari River Basin (Bolivia). *Water* **2022**, *14*, 3750. [CrossRef]
21. Roche, M.A.; Bourges, J.; Cortes, J.; Mattos, R. *IV. CLIMATOLOGY AND HYDROLOGY IV.1. Climatology and Hydrology of the Lake Titicaca Basin*; Kluwer Academic Publishers: Dordrecht, The Netherlands, 1992.
22. Pillco Zolá, R.; Bengtsson, L.; Berndtsson, R.; Martí-Cardona, B.; Satgé, F.; Timouk, F.; Bonnet, M.P.; Mollericon, L.; Gamarra, C.; Pasapera, J. Modelling Lake Titicaca's Daily and Monthly Evaporation. *Hydrol. Earth Syst. Sci.* **2019**, *23*, 657–668. [CrossRef]
23. World Lake Database: International Lake Environment Committee (ILEC) Lago Titicaca (Lake Titicaca). Available online: https://wldb.ilec.or.jp/Display/html/3389 (accessed on 2 April 2024).
24. Erickson, C.L. *The Lake Titicaca Basin: A Pre-Columbian Built Landscape*; De Gruyter: Berlin, Germany, 2000.
25. Guédron, S.; Delaere, C.; Fritz, S.C.; Tolu, J.; Sabatier, P.; Devel, A.L.; Heredia, C.; Vérin, C.; Alves, E.Q.; Baker, P.A. Holocene Variations in Lake Titicaca Water Level and Their Implications for Sociopolitical Developments in the Central Andes. *Proc. Natl. Acad. Sci. USA* **2023**, *120*, e2215882120. [CrossRef] [PubMed]
26. Garreaud, R.; Vuille, M.; Clement, A.C. The Climate of the Altiplano: Observed Current Conditions and Mechanisms of Past Changes. *Palaeogeogr. Palaeoclimatol. Palaeoecol.* **2003**, *194*, 5–22. [CrossRef]
27. Revollo, M.M. Management Issues in the Lake Titicaca and Lake Poopo System: Importance of Developing a Water Budget. *Lakes Reserv. Res. Manag.* **2001**, *6*, 225–229. [CrossRef]

28. Agramont, A.; Craps, M.; Balderrama, M.; Huysmans, M. Transdisciplinary Learning Communities to Involve Vulnerable Social Groups in Solving Complex Water-Related Problems in Bolivia. *Water* **2019**, *11*, 385. [CrossRef]
29. Vera Cartas, J.; Pucheu, K.S.; Torres Beristain, B. Contributions towards an Ecosystem Based Management of Lake Titicaca. *Aquat. Ecosyst. Health Manag.* **2013**, *16*, 240–247. [CrossRef]
30. Foer, J. The The Island-Dwelling Uros of Lake Titicaca: Visiting a Misunderstood Tourist Trap. Available online: https://www.slate.com/articles/life/world_of_wonders/2011/02/the_island_people.html (accessed on 4 April 2024).
31. Dejoux, C.; Iltis, A. *Lake Titicaca: A Synthesis of Limnological Knowledge*; Kluwer Academic Publishers: Dordrecht, The Netherlands, 1992.
32. Agramont, A.; van Cauwenbergh, N.; van Griesven, A.; Craps, M. Integrating Spatial and Social Characteristics in the DPSIR Framework for the Sustainable Management of River Basins: Case Study of the Katari River Basin, Bolivia. *Water Int.* **2022**, *47*, 8–29. [CrossRef]
33. Lazzaro, X.; Lamy, D. Accelerated Eutrophication in Lake Titicaca: Historical Evolution, Mechanisms, Monitoring, and Observatory Approach. In Proceedings of the International colloquium on current and ancient contamination in Andean aquatic ecosystems, La Paz, Bolivia, 3–5 May 2016.
34. Monroy, M.; Maceda-Veiga, A.; de Sostoa, A. Metal Concentration in Water, Sediment and Four Fish Species from Lake Titicaca Reveals a Large-Scale Environmental Concern. *Sci. Total Environ.* **2014**, *487*, 233–244. [CrossRef]
35. Dialogo Chino: Indigenous Women Lead Defence of Lake Titicaca's Dying Life. Available online: https://dialogochino.net/en/climate-energy/57223-indigenous-women-lead-defence-of-lake-titicacas-dying-life/ (accessed on 4 April 2024).
36. Stelzer, K.; Müller, D.; Simis, S.; Selmes, N. *Copernicus Global Land Operations "Cryosphere and Water" "CGLOPS-2": Quality Assessment Report*; Copernicus: European Union: Brussels, Belgium, 2020.
37. Simis, S.; Liu, X.; Crétaux, J.-F.; Yésou, H.; Malnes, E.; Blanco, P.; Merchant, C.; Carrea, L.; Duguay, C.; Wu, Y. *Product Validation and Algorithm Selection Report (PVASR) and Algorithm Development Plan (ADP)*; ESA: Paris, France, 2022.
38. Estado Peruano: Información Institucional - Autoridad Nacional Del Agua. Available online: https://www.gob.pe/institucion/ana/institucional (accessed on 15 October 2023).
39. Sharma, S.; Gray, D.K.; Read, J.S.; O'Reilly, C.M.; Schneider, P.; Qudrat, A.; Gries, C.; Stefanoff, S.; Hampton, S.E.; Hook, S.; et al. A Global Database of Lake Surface Temperatures Collected by in Situ and Satellite Methods from 1985–2009. *Sci. Data* **2015**, *2*, 150008. [CrossRef]
40. Molland, A.F. The Marine Environment. In *The Maritime Engineering Reference Book*; Elsevier: Amsterdam, The Netherlands, 2008; pp. 1–42. [CrossRef]
41. Copernicus Climate Change Service, Climate Data Store Lake Surface Water Temperature from 1995 to Present Derived from Satellite Observations. ECMWF: Reading, UK, 2020. [CrossRef]
42. Tyler, A.; Hunter, P.; De Keukelaere, L.; Ogashawara, I.; Spyrakos, E. Remote Sensing of Inland Water Quality. In *Encyclopedia of Inland Waters*, 2nd ed.; Elsevier: Amsterdam, The Netherlands, 2022; Volume 4, pp. 570–584. [CrossRef]
43. Wang, C.; Liu, J.; Qiu, C.; Su, X.; Ma, N.; Li, J.; Wang, S.; Qu, S. Identifying the Drivers of Chlorophyll-a Dynamics in a Landscape Lake Recharged by Reclaimed Water Using Interpretable Machine Learning. *Sci. Total Environ.* **2024**, *906*, 167483. [CrossRef] [PubMed]
44. Carrea, L.; Merchant, C. *Algorithm Theoretical Basis Document—Lake Surface Water Temperature 1km Products*; Copernicus: European Union: Brussels, Belgium, 2020.
45. Simis, S.; Stelzer, K.; Muller, D.; Selmes, N. *Algorithm Theoretical Basis Document—Lake Waters 300m and 1km Products*; Copernicus: European Union: Brussels, Belgium, 2020.
46. Simis, S.; Carrea, L.; Calmettes, B.; Cretaux, J.-F.; Duguay, C.; Liu, X.; Mangili, A.; Muller, D.; Yesou, H. *Lakes_CCI+-Phase 2. D2.2. Algorithm Theoretical Basis Document (ATBD)*; ESA: Paris, France, 2023.
47. Stelzer, K.; Simis, S.; Muller, D. *Copernicus Global Land Operations "Cryosphere and Water" Product User Manual—Lake Waters 300m and 1km Products*; Copernicus: European Union: Brussels, Belgium, 2020.
48. Carrea, L.; Merchant, C. *Copernicus Global Land Operations "Cryosphere and Water" Product User Manual—Lake Surface Water Temperature 1km Products*; Copernicus: European Union: Brussels, Belgium, 2020.
49. Carrea, L.; Crétaux, J.-F.; Liu, X.; Wu, Y.; Bergé-Nguyen, M.; Calmettes, B.; Duguay, C.; Jiang, D.; Merchant, C.J.; Mueller, D.; et al. ESA Lakes Climate Change Initiative (Lakes_cci): Lake Products, Version 2.0.2 2022.
50. Carlson, R.E. A Trophic State Index for Lakes. *Limnol. Oceanogr.* **1977**, *22*, 361–369. [CrossRef]
51. Woo, H.J.; Park, K.A. Inter-Comparisons of Daily Sea Surface Temperatures and in-Situ Temperatures in the Coastal Regions. *Remote Sens.* **2020**, *12*, 1592. [CrossRef]
52. Gillies, S.; Stewart, A.; Snow, A.; Culquicondor, A.; Amici, A.; Shepherd, A.; Ivanov, A.; Mountfield, A.; Kapadia, A.; Giardini, A.; et al. Rasterio: Geospatial Raster I/O for Python Programmers 2013. Available online: https://github.com/rasterio/rasterio (accessed on 15 February 2024).
53. Harris, C.R.; Millman, K.J.; Van Der Walt, S.J.; Gommers, R.; Virtanen, P.; Cournapeau, D.; Wieser, E.; Taylor, J.; Berg, S.; Smith, N.J.; et al. Array Programming with NumPy. *Nature* **2020**, *585*, 357–362. [CrossRef] [PubMed]
54. Ministerio de Desarrollo Sostenible y Medio Ambiente, Bolivia Reglamento En Materia de Contaminación Hídrica 1995.
55. Ministerio del Ambiente—MINAM, Peru Aprueban Estándares de Calidad Ambiental (ECA) Para Agua y Establecen Disposiciones Complementarias 2017.

56. Hirsch, R.M.; Slack, J.R.; Smith, R.A. Techniques of Trend Analysis for Monthly Water Quality Data. *Water Resour. Res.* **1982**, *18*, 107–121. [CrossRef]
57. Yue, S.; Wang, C.Y. Applicability of Prewhitening to Eliminate the Influence of Serial Correlation on the Mann-Kendall Test. *Water Resour. Res.* **2002**, *38*, 4-1–4-7. [CrossRef]
58. Raghul, M.; Porchelvan, P. An Approach for Monitoring Chlorophyll-A and Turbidity Levels in Saduperi and Kaveripakkam Lakes Located in and Around Vellore Region, Tamil Nadu, India, Using Spectral Unmixing Technique. *J. Indian Soc. Remote Sens.* **2024**. [CrossRef]
59. Albanai, J.A.; Karam, Q.; Ali, M.; Annabi-Trabelsi, N. Physicochemical Factors Affecting Chlorophyll-a Concentrations in the North-Western Arabian Gulf and Kuwait's Territorial Waters. *Arab. J. Geosci.* **2022**, *15*, 1671. [CrossRef]
60. Shourov, M.M.H.; Mahmud, I.; Niemeyer, K. NonStopAggroPop Mmhs013/pyMannKendall: V1.4.3 2023.
61. Zhou, J.; Leavitt, P.R.; Zhang, Y.; Qin, B. Anthropogenic Eutrophication of Shallow Lakes: Is It Occasional? *Water Res.* **2022**, *221*, 118728. [CrossRef] [PubMed]
62. INRENA Lake Titicaca. Available online: https://whc.unesco.org/en/tentativelists/5080/ (accessed on 25 August 2024).
63. Bartram, J.; Ballance, R.; UNEP; Weltgesundheitsorganisation (Eds.) *Water Quality Monitoring: A Practical Guide to the Design and Implementation of Freshwater Quality Studies and Monitoring Programmes*, 1st ed.; E & FN Spon: London, UK, 1996; ISBN 978-0-419-22320-7.
64. Chapman, D.V. (Ed.) *Water Quality Assessments: A Guide to the Use of Biota, Sediments and Water in Environmental Monitoring*, 2nd ed.; E & FN Spon: London, UK, 1996; ISBN 978-0-419-21590-5.
65. MacQuarrie, P.R.; Welling, R.; Aguirre, M. *Lake Titicaca Basin: Peru and Bolivia, Enhancing Transboundary Cooperation Through Technical Coordination and Institutional Reforms*; IUCN: Gland, Switzerland, 2013.
66. Matthews, M.W.; Bernard, S.; Robertson, L. An Algorithm for Detecting Trophic Status (Chlorophyll-a), Cyanobacterial-Dominance, Surface Scums and Floating Vegetation in Inland and Coastal Waters. *Remote Sens. Environ.* **2012**, *124*, 637–652. [CrossRef]
67. Attiah, G.; Kheyrollah Pour, H.; Scott, K.A. Lake Surface Temperature Retrieved from Landsat Satellite Series (1984 to 2021) for the North Slave Region. *Earth Syst. Sci. Data* **2023**, *15*, 1329–1355. [CrossRef]
68. Mao, Z.; Chen, J.; Hao, Z.; Pan, D.; Tao, B.; Zhu, Q. A New Approach to Estimate the Aerosol Scattering Ratios for the Atmospheric Correction of Satellite Remote Sensing Data in Coastal Regions. *Remote Sens. Environ.* **2013**, *132*, 186–194. [CrossRef]
69. Castro, C.C.; Gómez, J.A.D.; Martín, J.D.; Sánchez, B.A.H.; Arango, J.L.C.; Tuya, F.A.C.; Díaz-Varela, R. An UAV and Satellite Multispectral Data Approach to Monitor Water Quality in Small Reservoirs. *Remote Sens.* **2020**, *12*, 1514. [CrossRef]
70. MacCallum, S.N.; Merchant, C.J. Surface Water Temperature Observations of Large Lakes by Optimal Estimation. *Can. J. Remote Sens.* **2012**, *38*, 25–45. [CrossRef]
71. Ruiz-Verdu, A.; Jiménez, J.C.; Lazzaro, X.; Tenjo, C.; Delegido, J.; Pereira, M.; Sobrino, J.A.; Moreno, J. Comparison of MODIS and Landsat-8 Retrievals of Chlorophyll-A and Water Temperature over Lake Titicaca. In Proceedings of the International Geoscience and Remote Sensing Symposium (IGARSS) 2016, Beijing, China, 10–15 July 2016; pp. 7643–7646. [CrossRef]
72. Archundia, D.; Duwig, C.; Spadini, L.; Uzu, G.; Guédron, S.; Morel, M.C.; Cortez, R.; Ramos Ramos, O.; Chincheros, J.; Martins, J.M.F. How Uncontrolled Urban Expansion Increases the Contamination of the Titicaca Lake Basin (El Alto, La Paz, Bolivia). *Water Air Soil Pollut.* **2016**, *228*, 44. [CrossRef]
73. BID Programa de Saneamiento Del Lago Titicaca (Cuenca Katari, Bahía Cohana): Analisis Ambiental y Social (AAS). Available online: https://ewsdata.rightsindevelopment.org/files/documents/18/IADB-BO-L1118_PbsvUa3.pdf (accessed on 7 October 2024).
74. Stelzer, K.; Simis, S.; Müller, D. *Product User Manual—Lake Waters 300m and 1km Products*; Copernicus: European Union: Brussels, Belgium, 2020.
75. Baltodano, A.; Agramont, A.; Lekarkar, K.; Spyrakos, E.; Reusen, I.; van Griensven, A. Exploring Global Remote Sensing Products for Water Quality Assessment: Lake Nicaragua Case Study. *Remote Sens. Appl. Soc. Environ.* **2024**, *36*, 101331. [CrossRef]
76. Aguilar-Lome, J.; Soca-Flores, R.; Gómez, D. Evaluation of the Lake Titicaca's Surface Water Temperature Using LST MODIS Time Series (2000–2020). *J. South Am. Earth Sci.* **2021**, *112*, 103609. [CrossRef]
77. Vargas-Cuentas, N.I.; Roman-Gonzalez, A. Analysis of Harmful Algal Blooms in Lake Titicaca Using Remote Sensing. In Proceedings of the International Astronautical Congress 2019, Washington, DC, USA, 21–25 October 2019.
78. Siegel, D.A.; Behrenfeld, M.J.; Maritorena, S.; McClain, C.R.; Antoine, D.; Bailey, S.W.; Bontempi, P.S.; Boss, E.S.; Dierssen, H.M.; Doney, S.C.; et al. Regional to Global Assessments of Phytoplankton Dynamics from the SeaWiFS Mission. *Remote Sens. Environ.* **2013**, *135*, 77–91. [CrossRef]
79. Meals, D.; Spooner, J.; Dressing, S.; Harcum, J. *Statistical Analysis for Monotonic Trends, Tech Notes 6, November 2011*; Developed for U.S. Environmental Protection Agency by Tetra Tech, Inc.: Fairfax, VA, USA, 2011.
80. Tuladhar, D.; Dewan, A.; Kuhn, M.; Corner, R.J. The Influence of Rainfall and Land Use/Land Cover Changes on River Discharge Variability in the Mountainous Catchment of the Bagmati River. *Water* **2019**, *11*, 2444. [CrossRef]